Intratumoral Treg ablation is sufficient to mediate tumor control systemically without autoimmunity

Alissa Bockman[1], Brenna Gittins[1], Chenyu Zhang[1], Jessica Hung[1], Mariela Moreno Ayala[1], Dorothée Saddier Axe[2], Brian M Weist[2], Michel DuPage[1]
[1]Division of Immunology & Molecular Medicine, Department of Molecular & Cell Biology, University of California, Berkeley;
[2]Gilead Sciences, Inc., 333 Lakeside Drive, Foster City, CA 94404, USA

Contact: dupage@berkeley.edu

ABSTRACT

Regulatory T cells (T_{regs}) infiltrate most tumors, yet whether they suppress immune responses directly within tumor tissues is not clear. We used intratumoral (IT) delivery of diphtheria toxin (DT) in *Foxp3*^{DTR} mice to deplete IT T_{regs} while leaving peripheral T_{regs} intact. IT delivery of DT reduced T_{reg} frequencies in the tumor, which promoted potent tumor control without autoimmunity. Interestingly, this control was principally mediated by CD4$^+$ T cells, whereas CD8$^+$ T cells only contributed when CD4$^+$ T cells were absent. While conventional dendritic cells (cDCs) were required to clear tumors, Batf3$^+$ cDC1s were dispensable. Distant secondary tumors, mimicking metastases, were also controlled by IT T_{reg} ablation. Mechanistically, IT T_{regs} suppressed antitumor T cell responses by blocking the acquisition of tumor antigen by cDC2s. Importantly, similar mechanisms of control were observed using a clinically translatable IT T_{reg}-depleting anti-CCR8 antibody and reveal a distinct therapeutic strategy that leverages cDC2s and CD4$^+$ T cells.

INTRODUCTION

High frequencies of tumor-infiltrating regulatory T cells (T_{regs}) are correlated with reduced survival in cancer patients[1–6]. T_{regs} inhibit immune responses through the secretion of suppressive cytokines and the inhibition of costimulatory ligand expression on APCs, among other suppressive mechanisms[7–10]. Eliminating T_{regs} as a therapy is complicated by the fact that T_{regs} are essential for preventing harmful inflammation, including autoimmunity[11–14]. Therefore, to target T_{regs} for the treatment of cancer will require approaches that only disrupt T_{reg} suppression of antitumor immunity while retaining T_{reg} immunoregulatory function in non-tumor tissues.

One approach would be the selective depletion of T_{regs} within tumors, but studies have suggested that T_{regs} may suppress antitumor immune responses outside of the tumor microenvironment[15–19]. Nevertheless, antibody-based strategies that selectively deplete intratumoral (IT) T_{regs} have worked well in mouse models, for example, with antibodies that can deplete intratumoral T_{regs} by targeting CTLA-4, CD25, GITR, 4-1BB, OX-40, LAG3, TIGIT orCCR4[5,10,20–275,10,20–26]. Most recently, T_{regs} were found to upregulate the chemokine receptor CCR8 in tumors from humans and mice[28–32], leading to experiments showing that anti-CCR8 antibodies can effectively control

several types of cancer in mice[33–38]. Currently, phase I and II clinical trials with anti-CCR8 are underway for advanced and metastatic solid cancers (NCT05537740; NCT05101070; NCT06387628; NCT05007782; NCT05635643; NCT05935098). Despite the promise of these new antibody approaches that can selectively deplete IT T_{regs}, the fundamental question as to whether T_{regs} suppressive function occurs only in tumors is not resolved. That is because such antibody approaches cannot be solely restricted to tumor tissues, as cells outside of tumors expressing the target antigen (i.e. CCR8), which include non-T_{reg} cells, may also contribute to tumor control[39–41]. Furthermore, the activation of Fc receptors on immune cells that engage therapeutic antibodies may be critical for the efficacy of these therapeutics[27,42–4442–44]. Therefore, further research into T_{reg} depletion without using antibodies will directly test whether IT T_{reg} ablation alone directs anti-tumor immunity.

To prevent the activity of antibodies binding to cells outside of the tumor microenvironment, investigators have performed IT delivery of antibodies, as well as immune adjuvants CpG and IL-12-Fc[45–48]. Direct, intratumoral TLR9 activation by CpG injection promoted the control of treated tumors as well as untreated tumors[45]. When TLR9/CpG administration was combined with anti-CTLA4 or anti-OX40 to deplete IT T_{regs}, therapeutic activity was enhanced, leading to effective control of both treated tumors as well as disseminated tumors[45–48]. Intratumoral immunotherapy poses significant clinical benefit, as local delivery may mitigate the autoimmune toxicities that are elicited by systemic drug administrations[49]. However, the role of Fc receptor binding and immune cell activation are still likely to be important, and alternative methods that do not employ antibodies to remove intratumoral T_{regs} must be tested[50].

To directly test whether T_{reg} ablation only within tumors is sufficient to control tumors without inciting autoimmunity, we delivered a low dose of diphtheria toxin directly into tumor tissues by intratumoral diphtheria toxin injection (IT DT) in *FoxP3*^{DTR} mice[11,51]. This technique led to nearly complete ablation of IT T_{regs} while sparing T_{regs} at peripheral sites throughout the mice. While others have used higher doses of IT DT to ablate tdLN and IT T_{regs}, here we establish a lower dose DT strategy in which IT T_{regs} are ablated with minimal tdLN T_{reg} depletion[27]. Most importantly, IT T_{reg} ablation by itself led to potent tumor control without inciting autoimmune disease. Furthermore, the ablation of T_{regs} from a single tumor led to control of distant tumors of the same origin that did not receive direct treatments. Unexpectedly, tumor control was dominantly mediated by $CD4^+$ T conventional (Tconv) cells rather than $CD8^+$ T cells, although $CD8^+$ T cells did contribute to tumor control in the absence of $CD4^+$ T cells. In addition, cDC1s were not required for tumor control with IT T_{reg} ablation. Mechanistically, we show that IT T_{regs} suppressed the antitumor response locally by blocking the acquisition of tumor antigen by cDC2s within tumors. We demonstrate enhanced antigen acquisition by cDC2s upon the removal of IT T_{reg} suppression. Similar cell type dependencies were observed with clinically applicable anti-CCR8 intratumoral T_{reg} depleting antibodies. These findings are consequential, as they

uncover a clinically relevant mechanism to boost systemic antitumor immune responses that does not rely on $CD8^+$ T cells or cDC1s and is effective without inciting autoimmune toxicity.

RESULTS

Intratumoral T_{reg} depletion controls tumor growth without inciting autoimmunity

It is unclear whether approaches to deplete intratumoral (IT) T_{regs} selectively would have clinical efficacy, as systemic T_{reg} depletion has almost exclusively been tested[52–54]. Several reports have shown that T_{reg} depletion outside of the tumor, e.g. in tumor-draining lymph nodes, is critically important for tumor control[15,16,18,55]. However, recent work has also shown that anti-CCR8 antibodies, which deplete T_{regs} selectively within tumors, prolong mouse survival after challenge with subcutaneously implanted CT26 colorectal carcinoma or EMT6 breast cancer cell lines[33,34]. We confirmed previous findings that T_{regs} within MC38 tumors highly express CCR8, and that anti-CCR8 treatment reduces $CCR8^+$ IT T_{reg} numbers in tumors and significantly decreases MC38 tumor burden (Fig. S1A-G)[28,29,35,37]. Interestingly, anti-CCR8 treatments were not effective against B16F10 tumors (Fig. S1F-G). Overall, these data were consistent with an important role for the local activity of IT T_{regs} in mediating tumor immunotolerance. However, because CCR8 can be expressed on a subset of circulating T_{regs} and $CD4^+$ T conv cells, it remained possible that anti-CCR8 therapy exerted tumor control by acting more broadly than on IT T_{regs} alone. Furthermore, antibody-mediated cell depletion that activates Fc receptors may have also contributed to the antitumor efficacy[43]. To test whether IT T_{reg} ablation alone is sufficient to promote tumor control without the use of antibodies, we used *FoxP3*^{DTR} mice. However, rather than deliver diphtheria toxin (DT) systemically by intraperitoneal (IP) injection, we delivered low dose DT (250 ng, one-fourth of the dose used IP) directly into tumors (IT) every other day once tumors reached a volume of 50 mm^3 and as long as tumors were palpable (Fig. 1A). After a single dose of IT DT, IT T_{regs} were efficiently depleted by 48 hours (Fig. 1B). Importantly, we found that IT DT ablation of IT T_{regs} induced significant control of both immune-rich MC38 tumors and poorly immunogenic B16F10 tumors. As IT DT treatment was stopped after complete tumor regression occurred, we found that no tumors rebounded upon cessation of treatment (Fig. 1C,1D).

To determine if IT T_{reg} ablation also promotes tumor control in autochthonous models of cancer, we induced sarcomas in *K-ras*$^{LSL\text{-}G12D}$*;p53*$^{fl/fl}$ ('KP') mice that were bred to the *FoxP3*^{DTR} allele[56]. We dosed *FoxP3*^{DTR}*;K-ras*^{G12D}*;p53*$^{fl/fl}$ with 50,000 infectious units of a lentivirus encoding Cre recombinase (Lenti-x) into the left calf muscle[57,58]. Over the following 150 days, we monitored mice for spontaneous tumor development. When tumors became palpable, mice were administered IT DT as with subcutaneous tumors. We found that IT DT resulted in a significant reduction of IT T_{regs} in this autochthonous tumor setting (Fig. 1E). Ultimately, this reduction in IT T_{regs} was sufficient to extend animal survival, despite the aggressive nature of this tumor model (Fig. 1F). Importantly, Lenti-x-induced sarcomas lack neoantigens recognized by $CD8^+$ T cells and were previously categorized as poorly immunogenic[57,58]. Therefore, IT T_{reg} ablation

appeared to promote immune control in a manner independent of a $CD8^+$ T cell response. These results demonstrate a tumor-protective function of IT T_{regs} that is conserved across multiple cancer models.

While we observed robust control of IT T_{reg} ablated tumors, we sought to address whether IT T_{reg} ablation also prevented the induction of autoimmune pathologies observed with systemic T_{reg} ablation[11–14,59]. We directly compared *FoxP3*^{DTR} tumor-bearing mice treated with IT DT versus IP DT for a period of 28 days by measuring T_{reg} frequencies, autoimmune pathologies, and the activation status of conventional T cells. First, IP DT treatment induced a significant reduction in T_{reg} frequencies across all tissues analyzed, whereas IT DT impacted T_{reg} frequencies predominantly within the tumor tissue, albeit a moderate T_{reg} reduction was observed in the tumor-draining lymph node (tdLN) (Fig. 2A and Fig. S2A). Second, IP DT treatments significantly increased spleen weight and caused body weight loss in mice with tumors, but IT DT did not (Fig. 2B-C; Fig. S2B-C). Furthermore, analysis of hematoxylin and eosin stained sections from the lung, liver, kidney, and heart of IP DT treated mice revealed significant lymphocytic infiltration that was not observed in mice receiving IT DT (Fig. 2D-E, Fig. S2D-E). Third, flow cytometric analysis of $CD4^+$ Tconv and $CD8^+$ T cells from IP DT treated mice, but not IT DT treated mice, revealed robust increases in the expression of CD44, ICOS, CD25, PD1 and TIGIT in the spleen, non-draining lymph nodes (ndLN) and tdLN (Figures 2F-G; Fig. S2F-G). Interestingly, while IT T_{reg} ablation did not induce any sign of systemic autoimmunity, IT T_{reg} ablation did produce more durable and complete rejections (CRs) of tumors compared to systemic T_{reg} ablation by IP DT (Fig. S2H-I). These data demonstrate that IT T_{reg} ablation can control tumors without inducing aberrant immune activation or multi-organ autoimmune disease.

Intratumoral T_{reg} depletion promotes $CD8^+$ and $CD4^+$ T cell activation locally in tumors

We next characterized the immunological changes within MC38 tumors after IT T_{reg} ablation. While the frequency of $CD4^+$ Tconv cells trended slightly higher with IT T_{reg} ablation, the difference was not statistically significant after 25 days of IT T_{reg} ablation (Fig. 3A). However, we did observe a significant increase in the frequency of $CD8^+$ T cells, as observed by others with anti-CCR8 treatment[28,33]. To determine whether IT T_{reg} ablation also increased the frequency of tumor-reactive $CD8^+$ T cells, we stained single cell suspensions collected from IT DT treated tumors with a tetramer specific for the p15E peptide of an endogenous ecotropic murine leukemia virus to detect MC38-specific $CD8^+$ T cells. As has been reported for anti-CCR8 treatments[15,28,34,60–62], we also observed a trend of an increased frequency of $p15E^+CD8^+$ T cells in tdLNs after IT T_{reg} ablation, but the increase in tumor tissues did not reach significance (Fig. S3A-B). We also noted an increase in effector (CD44+CD62L-) $CD4^+$ and $CD8^+$ T cells in tumor tissue after IT DT (Fig. 3B). We found that IT T_{reg} ablation induced significant upregulation of ICOS and CD25 on IT $CD4^+$ Tconv cells (Fig. 3C and Fig. S3C) and $CD8^+$ T cells (Fig. 3D and Fig. S3D). While the production of TNFα and IFNγ by tumor-infiltrating $CD4^+$ and $CD8^+$ T cells was similar between IT PBS and IT DT treated mice (Fig. 3F and Fig. S3E-I), we observed a

significant increase in the frequency of IL-2 producing $CD4^+$ Tconv cells after IT T_{reg} ablation (Fig. 3E and Fig. S3J). These results demonstrate that the removal of IT T_{regs} led to an increase in the activation status of conventional $CD4^+$ and $CD8^+$ T cells within tumor tissues.

To better understand whether the increase in T cells within tumors, observed after IT DT treatment, required the recruitment of T cells from the tdLN, we treated mice with a lymphocyte egress inhibitor (FTY720) when IT DT treatment began (D0). We found that mice treated with IT DT and FTY720 rejected tumors as efficiently as those treated with DMSO and IT DT (Fig. S3K). These data suggest that the increase in T cell frequency within IT DT treated tumors was due to the expansion and retention of T cells within tumors and not due to an influx of T cells from the tdLN. This also suggests that increased priming of T cells in lymphoid tissues is not required for tumor control with IT T_{reg} ablation. Therefore, we hypothesize that a reinvigorated T cell pool within tumor tissue itself is sufficient to promote the tumor control observed with IT T_{reg} ablation.

$CD4^+$ T conventional cells can control tumors after IT T_{reg} ablation

It is widely hypothesized that IT T_{reg} ablation unleashes $CD8^+$ T cells to control tumors[15,18,21,28,33,53,60,63]. To directly test the cellular requirements for tumor control after IT T_{reg} ablation with IT DT, we performed *in vivo* cellular depletion studies using antibodies against $CD4^+$ and $CD8^+$ T cells or natural killer (NK1.1+) cells with IT DT administration (Fig. 4A). Tumor control and survival with IT T_{reg} ablation was unaffected by either $CD8^+$ T cell or NK cell depletion alone (Fig. 4B-E and Fig. S4A-B). However, depletion of $CD4^+$ Tconv cells significantly impaired tumor control and survival with IT T_{reg} ablation. Interestingly, $CD8^+$ T cell depletion in combination with $CD4^+$ T cell depletion fully reversed tumor control with IT T_{reg} ablation. Thus, $CD4^+$ T cells played a primary role in tumor control with IT T_{reg} ablation, while $CD8^+$ T cells only appeared to be required for tumor control in the absence of $CD4^+$ T cells.

This led us to test whether anti-CCR8 treatment, which is presumed to activate $CD8^+$ T cell responses to tumors[28,33–37], also exhibited similar cellular requirements for tumor control. With anti-CCR8 treatment, tumor control and survival were not prevented by NK or $CD8^+$ T cell depletion alone, but were significantly reversed by depletion of $CD4^+$ T cells, exactly as observed with the IT DT approach (Fig. 4F-G and Fig. S4C). Again, $CD8^+$ T cells only participated in tumor control when $CD4^+$ T cells were also depleted. Thus, despite the robust infiltration and activation of $CD8^+$ T cells with IT T_{reg} ablation, $CD8^+$ T cells do not appear to play a primary role in tumor control on their own. Overall, our findings instead highlight the largely underappreciated role for $CD4^+$ T cells to control tumors without $CD8^+$ T cells, particularly in the context of IT T_{reg} ablation.

As dendritic cells are integral to initiating and maintaining T cell responses, we next interrogated whether conventional DCs (cDCs) were required for tumor control elicited by IT

T_{reg} ablation. We generated *Foxp3^{DTR};Zbtb46^{DTR}* mice and then used their bone marrow to make bone marrow chimeric mice in which T_{regs} and cDCs could be inducibly ablated with DT administration[64,65]. Bone marrow chimera mice are required with *Zbtb46^{DTR}* mice due to toxicity observed in intact *Zbtb46^{DTR}* mice[64]. We implanted tumors into these mice and began IT DT treatment once tumors reached ~50 mm^3 (Fig. 4H). Tumor control with IT DT was prevented in mice that lacked cDCs (Fig. 4I). We also found that, in the absence of all cDCs, the increased frequency of conventional T cells within tumors that we had observed with IT T_{reg} ablation was prevented (Fig. S4D). These results suggest that cDCs were required for increasing the infiltration or maintenance of T cells within tumor tissues upon IT T_{reg} ablation.

As cDC1s are well-established as being integral to antitumor immunity in several contexts, such as checkpoint blockade immunotherapies, we next tested whether Batf3$^+$, type I DCs (cDC1s) were required for tumor control with IT T_{reg} ablation[66–69]. We generated *FoxP3^{DTR};Batf3$^{-/-}$* mice and then used IT DT treatment to ablate IT T_{regs} in mice that constitutively lacked cDC1s. We found that cDC1-deficient mice controlled tumors equivalently to control mice (Fig. 4J; Fig. S4E). These data indicate that cDC1s are not important for controlling tumors upon IT T_{reg} ablation and may also support the dispensability for CD8$^+$ T cells previously observed. Notably, as a subset of cDC1s express CD8α, our previous experiments (Fig. 4A-G) selectively depleted CD8$^+$ T cells using anti-CD8β depleting antibodies, thereby leaving this subset of cDC1s intact. These results highlight the dispensability of cDC1s in our model andsuggest that cDC2s, which were left intact in *Batf3$^{-/-}$* mice, may be the critical subtype of cDC required for tumor control with IT T_{reg} ablation.

Ablation of IT T_{regs} in a single tumor unleashes antitumor immunity against distal tumors

As disseminated metastatic cancers are in greatest need of treatment and would not be easily treated by IT delivery of agents to all tumors, we wanted to determine whether IT T_{reg} ablation in a single tumor would also boost systemic antitumor immune responses that could control untreated tumors. A precedent exists to support this hypothesis, as local radiation and IT injection of TLR agonists or checkpoint blockade inhibitors have been shown to not only impact the treated tumor, but distal tumors as well[46,48]. To test whether IT T_{reg} ablation alone in a single tumor also imparts control of distal tumors, we inoculated syngeneic tumors on both flanks of *FoxP3^{DTR}* mice. We then initiated IT DT treatment in only one of the two tumors when the average volume of both tumors were ~50 mm^3. In mice with paired MC38 or B16F10 tumors, we found that IT DT treatment of one tumor in each mouse resulted in control of both the treated tumor and the untreated distal tumor (Fig. 5A,B and Fig. S5A-C). Control was only lost in distal tumors when DT treatment ceased due to the rejection of the primary treated tumors and our inability to continue IT DT treatments. Thus, IT T_{reg} ablation led to systemic control of a distal tumor even though distal tumors were not directly ablated of T_{regs}. These results were indicative of the potential efficacy of IT T_{reg} ablation in a single tumor also controlling distant metastases.

We hypothesized that the control of the untreated distal tumor resulted from enhanced T cell activation against tumor antigens in the treated tumor that led to a stronger systemic T cell response against the specific tumor, which could target distant untreated tumors due to shared tumor antigens. However, distal tumor control could also be induced if IT T_{reg} ablation led to enhanced inflammation that promoted distinct T cell responses in the distant tumor. To discern which mechanism contributed to distal tumor control, we inoculated individual *FoxP3*^{DTR} mice with two antigenically mismatched tumors, specifically MC38 on one flank and B16F10 on the other, and administered IT DT to only one tumor in each mouse (Fig. 5C). Unlike in mice with matched syngeneic tumors, in these mice with mismatched tumors, IT DT treatment only controlled the treated tumor and not the distal tumor (Fig. 5C). These results indicate that specific immunity generated within the treated tumor, likely reflecting T cell antigen specificity, contributed to the antitumor activity elicited against a distal, syngeneic tumor that was not directly treated. Furthermore, these results confirm that our IT DT approach results in local IT T_{reg} ablation that is restricted to the treated tumors and does not disrupt T_{regs} systemically, consistent with our finding that IT DT treatment does not induce systemic autoimmunity.

To investigate whether the T cell responses in distal untreated tumors were changed by IT T_{reg} ablation specifically with matched syngeneic tumors, we assessed the frequency and activation state of T cells in the tumors. In matched syngeneic tumors, there was a significant reduction of T_{regs} and an increase in activated ($CD44^+$) $CD8^+$ and $CD4^+$ Tconv cells in the untreated tumors (Fig. 5D). We also observed an upregulation of PD1 and downregulation of CD62L on both T cell subsets in untreated tumors (Fig. S5D-E). However, in mismatched tumors, changes in T_{reg} frequencies and conventional T cell activation status were not observed, supporting the hypothesis that tumor antigen-specific T cell responses were only coordinated in the case of the matched tumors (Fig. 5E, F, Fig. S5F).

Control of disseminated tumors is reversed by $CD8^+$ or $CD4^+$ T cell depletions

The impact of IT T_{reg} ablation on infiltration of $CD4^+$ and $CD8^+$ T cells into distant syngeneic tumors suggested that either or both of these populations may participate in distal tumor control. We therefore used cellular depletion studies to establish the immune cell dependencies for distal tumor control (Fig. 6A). As observed with single tumors, depletion of $CD4^+$ T cells reversed the control of the IT T_{reg} ablated tumors as well as the matched distal tumors (Fig. 6B). Interestingly, however, while depleting $CD8^+$ T cells alone did not impede the control of the primary treated tumors (as observed with single tumors, Fig. 4), control of the untreated distal tumor was largely reversed by $CD8^+$ T cell depletion (Fig. 6B). These results demonstrate a context-specific dependency for $CD8^+$ T cells in the control of primary versus disseminated cancer with IT T_{reg} ablation.

The requirement for $CD8^+$ T cells to control matched disseminated tumors may indicate different cDC requirements for primary versus distal tumor control with IT T_{reg} ablation. Therefore, we

again generated *Foxp3*^{DTR}*;Zbtb46*^{DTR} bone marrow chimera mice, implanted MC38 tumors on both flanks, and performed IT DT treatment of primary tumors (Fig. 6C). Conditional deletion of both IT T_{regs} and cDCs completely blocked the control of untreated distal tumors as well as the primary tumors (Fig. 6D). These data suggest that enhanced T cell activation observed after IT T_{reg} ablation is dependent upon the presence of cDCs. Given the requirement of $CD8^+$ T cells in controlling tumor progression at a distal site, we expected that cDC1s might contribute to the clearance of dual tumors. However, *FoxP3*^{DTR}*;Batf3*$^{-/-}$ mice with dual tumors and IT DT treatment of a primary tumor showed no impairment in the control of either tumor (Fig. 6E, F). Thus, cDCs that do not require Batf3 function were sufficient to promote tumor control with IT T_{reg} ablation, suggesting again that cDC2s may act as the critical mediators of primary and distal tumor control.

IT T_{reg} ablation enhances tumor antigen acquisition by cDC2s

To investigate how IT T_{reg} ablation impacted cDCs within the tumor, we implanted MC38 tumor cells that expressed an mCherry fluorescent protein as a trackable tumor antigen[67]. Additionally, we pre-depleted $CD8^+$ T cells in *FoxP3*^{DTR} mice prior to tumor implantation to reduce any complications due to $CD8^+$ T cell-mediated cytotoxicity in enhancing tumor antigen release. When tumors reached ~50 mm^3, we administered 3 doses of IT DT every other day and at day seven, tumors and tdLNs were analyzed by flow cytometry to quantify immune cells that had phagocytosed fluorescent tumor antigen, in particular cDC1s and cDC2s (Fig. 7A). We found a significant increase in the frequency of $mCherry^+$ $CD11c^+$MHC-II^+ DCs in the tumors but not tdLN of IT T_{reg} ablated mice (Fig. 7B and Fig. S6A). Interestingly, by further gating on $CD103^+$ cDC1s and $CD11b^+$ cDC2s, we observed that only the cDC2s exhibited significantly increased tumor antigen uptake in tumors upon IT T_{reg} ablation (Fig. 7C and Fig. S6B). In addition, as observed previously with systemic T_{reg} depletion[16,70–72], we observed increased expression of CD80 and CD86 costimulatory ligands on $CD11c^+$MHC-II^+ DCs, especially on DCs that were actively phagocytosing tumor antigen (i.e. $mCherry^+$) (Fig. S6C-E). Interestingly, however, we again observed that only the tumor antigen+ cDC2s, and not antigen+ cDC1s, exhibited increased expression of CD80 and CD86 ligands in tumors (Fig. 7D). This highlights a crucial role for IT T_{regs} in limiting cDC2 tumor antigen uptake and maturation in tumors, which likely leads to reduced antitumor $CD4^+$ and $CD8^+$ antitumor T cell responses.

To directly test whether cDC2s from tumors exhibited increased phagocytic capacity after IT T_{reg} ablation, we tested tumor single cell suspensions of tumors harvested from IT DT versus IT PBS treated mice for uptake of fluorescent beads *ex vivo* (Fig. 7E). In this assay, we again found that the primary subset of cDCs that had increased phagocytosis of bead antigen in the absence of IT T_{regs} were cDC2s, although IT T_{reg} ablation also enhanced bead uptake in cDC1s, but to a lesser extent (Fig. 7F). These data reveal a novel mechanism by which IT T_{regs} restrict antitumor T cell responses, by restricting tumor antigen uptake locally within tumors. Here, we demonstrate that IT T_{regs} restrict cDC2 uptake of tumor antigen within tumor tissue, thereby dampening $CD4^+$

Tconv cell responses against both local and disseminated tumors. By eliminating T_{regs} specifically within tumors, we found that cDC2 activation and phagocytic capacity were dramatically enhanced, unleashing a $CD4^+$ Tconv cell response that acts independently of cDC1s to control tumors. Thus, intratumoral T_{reg} ablation activates an alternative mechanism of tumor control that depends on cDC2s and $CD4^+$ Tconv cells.

DISCUSSION

Although modulating T_{reg} function is a key approach to boosting cancer immunotherapy, the role of intratumoral T_{regs} and the mechanisms by which they suppress anti-tumor T cell responses remains incompletely defined. To address this gap in knowledge, we leveraged the *FoxP3*^{DTR} mouse coupled with low-dose IT DT treatment to selectively ablate T_{regs} in tumors. These experiments revealed that T_{reg} ablation within tumor tissue itself was sufficient to limit tumor growth. Importantly, this tumor control occurred without any autoimmune side effects, which are common with T_{reg}-targeting approaches. Removal of IT T_{regs} increased conventional $CD4^+$ and $CD8^+$ T cell activation in tumors. However, $CD4^+$ Tconv cells and conventional type II dendritic cells (cDC2s) were the primary cells responsible for tumor control with IT T_{reg} ablation. These cellular requirements extended to clinical cancer interventions, as we also observed a requirement for $CD4^+$ Tconv cells, rather than $CD8^+$ T cells, after anti-CCR8 antibody-mediated IT T_{reg} depletion. These data are consequential, as many combinatorial therapeutics aimed at reducing T_{reg} suppression are thought to act by bolstering antitumor $CD8^+$ T cell responses[15,24,28,53,60,61]. For example, two recent studies specifically disrupted IT T_{regs}, even with anti-CCR8 antibodies, and showed increased frequencies of total and tumor-specific CD8+ T cells in tumors, as we also observed in this study, but did not functionally validate their importance by cellular depletion experiments[27,38]. Still other groups have disrupted intratumoral T_{reg} function through either targeting tumor-specific T_{reg} genes or disrupting their recruitment, and in these cases the mechanisms of tumor control were shown to be driven by $CD8^+$ T cell responses[63,67,73]. Here we show, by $CD8^+$ T cell depletion, that $CD8^+$ T cells are not required for tumor control, as previously hypothesized, and instead reveal the critical importance of $CD4^+$ Tconv cells for tumor control upon total IT T_{reg} ablation.

Here, we also established that systemic responses against disseminated cancers, e.g. metastases, is enhanced by IT T_{reg} ablation in a single tumor. Enhanced antitumor responses only occurred when we disrupted IT T_{reg} suppression in a tumor of the same origin as an untreated distal tumor. However, in this setting of disseminated cancer, we found that both $CD8^+$ and $CD4^+$ Tconv cells were essential for controlling untreated distal tumors. These findings align with other studies that demonstrated an abscopal therapeutic effect after local IT immunotherapies[46,47,60], but extend such findings by revealing the importance of cDC2s and $CD4^+$ Tconv cells in the control of distal and untreated tumors. Further, our findings are unique in showing that systemic immune responses can be elicited by antibody-independent, non-Fc receptor activating, depletion of IT T_{regs}.

By disrupting conventional DCs, we also uncovered a critical role for cDCs in promoting T cell responses against tumors. Most cancer immunotherapeutic studies have focused on the role of cDC1s in promoting T cell responses to tumors[74–77]. As such, efforts have focused on targeting the cDC1-CD8 T cell axis in human cancer immunotherapies, such as by selectively disrupting T_{reg} interactions with cDC1s[67]. However, as IT T_{reg} ablated tumors appear to require $CD4^+$ Tconv cell responses, it is possible that a different subset of conventional DCs are important for tumor control in this setting. Indeed, while CXCR3+ T_{regs} were shown to selectively impede $CD8^+$ T cell responses against tumors, our data demonstrate that removal of all IT T_{regs} induces tumor regression through a cDC2, and cDC1-independent, mechanism. Recent literature has demonstrated that mature DCs enriched in immunoregulatory molecules (mregDCs) can recruit T_{regs}, allowing for their accumulation around lymphatic vessels in the peripheral tumor stroma[78]. By disrupting this mregDC-T_{reg} axis, tumor immunosurveillance was enhanced[79]. While our data suggest a prominent role for cDC2s in stimulating anti-tumor immune activity, it remains possible that mregDCs may also contribute to tumor rejection in the absence of T_{regs}. Together, these findings are consequential, as they represent a parallel arm of antitumor T cell immune function that may bolster tumor control in cDC1 or $CD8^+$ T cell non-responsive tumors.

We also show that IT T_{regs} blocked the acquisition of tumor antigens by cDC2s within tumor tissue. In the absence of all cDCs, we abrogated enhanced T cell activation and expansion induced by IT T_{reg} ablation. Recently, Binnewies et. al. demonstrated a critical role for cDC2 responses in the tdLN after systemic T_{reg} removal[17]. These studies demonstrated that in the absence of T_{regs}, cDC2s drove stronger $CD4^+$ T cell responses by enhancing the trafficking of cDCs presenting tumor-derived antigens to $CD4^+$ Tconv cells in the tdLN[17,80]. Furthermore, a correlation between the abundance of IT cDC2s and the accumulation of IT$CD4^+$ Tconv cells was demonstrated in the absence of T_{regs}[68]. However, whereas previous studies have suggested that the migration of cDC2s is regulated by T_{regs}, here we show that the uptake of tumor antigens is also controlled by IT T_{regs}, and that regulation by cDC2s is important directly within tumors. That is because, unlike others[17], we found that FTY720 treatment did not impede tumor control with IT T_{reg} ablation, strongly suggesting that increased priming of $CD4^+$ T cells in tdLNs is not required for the efficacy of IT T_{reg} ablation. This may be due to the impact of IT-specific Treg ablation performed here, as opposed to systemic T_{reg} ablation, and deserves further investigation. In addition, it is noteworthy that IT T_{reg} ablation was beneficial compared to systemic T_{reg} ablation because it was sufficient to promote tumor control without causing autoimmune pathology commonly observed in other studies.

Maintenance of immune homeostasis is a vital function of T_{regs}[7,13]. Thus, disrupting global T_{reg} function incurs severe autoimmune disease in humans and in mice[11,12,14]. This motivated our efforts to locally deplete T_{regs} only in tumors to see if this was sufficient for tumor control and would retain critical T_{reg} suppressive functions in peripheral tissues. While others have employed

similar approaches to disrupt tdLN and tumor T_{regs} simultaneously[27], or use anti-CTLA4 targeting antibodies to disrupt IT T_{reg} function[43], our approach remains distinct as we only target IT-T_{regs} without the use of Fc-engaging antibodies and show tumor control likely occurred without tdLN T cell priming by use of FTY720. However, even though we did not detect changes in $CD4^+$ Tconv or $CD8^+$ T effector function within the tdLN, and tumor control was retained even with FTY720 treatment, it remains possible that low-level depletion of tdLN T_{regs} also contributed to antitumor immunity. However, our data that show a loss of tumor control when distant tumors are mismatched from the treated tumor does suggest that IT T_{reg} ablation acts locally within tumors. Thus, our results support the feasibility of strategies that selectively disrupt IT T_{regs} for safe and effective cancer immunotherapy.

Current clinical data demonstrate poor prognostic outcomes in tumors that are cDC1 or $CD8^+$ T cell low[81,82]. These tumors have been shown to respond poorly to anti-PD-1 checkpoint blockade as well as other immunotherapies[77,83,84]. In these cases, failed tumor immunosurveillance was attributed to the downregulation of MHC I molecules on the tumor cell surface, or the absence of tumor neoantigens, capable of eliciting CD8 T cell responses[85–88]. Our data identify a novel mechanism to combat CD8-resistant tumors, or synergize with such existing therapeutic strategies, by unleashing cDC2s and $CD4^+$ Tconv cell-mediated tumor control by IT T_{reg} ablation.

In summary, here we show that IT T_{reg} ablation is sufficient to promote tumor control and uncover a novel function of IT T_{reg} function - to suppress cDC tumor antigen uptake. IT T_{reg} function suppresses effective $CD4^+$ Tconv cell responses locally in tumors and disrupts the ability of both $CD4^+$ and $CD8^+$ T cells to cooperate in the control of distant untreated tumors. Our findings also extend to a clinically viable mode of IT T_{reg} depletion using an anti-CCR8 antibody delivered systemically. These data are consequential, as they demonstrate a novel arm of adaptive immunity that can be leveraged to enhance the immunotherapeutic treatment of patients with cancer.

Methods

All of the experiments were conducted according to the Institutional Animal Care and Use Committee guidelines of the University of California, Berkeley. Further information on the committees that approved protocols used in this publication can be found in each corresponding section.

In vivo animal studies

Mice used were bred onto a C57BL/6 background for a minimum of ten generations. Littermates or age-matched control mice (8-20 weeks old) were used in all mouse experiments. *Foxp3*$^{GFP\text{-}DTR}$ mice express human diphtheria toxin receptor and EGFP genes from the Foxp3 locus without disrupting expression of the endogenous FoxP3 gene[11]. These mice were a gift from Dr. Rudensky (Memorial Sloan Kettering Institute; JAX:016958). *Foxp3*$^{GFP\text{-}DTR}$*;Kras*^{G12D}*;p53*$^{fl/fl}$ mice were kindly provided by Dr. Jacks (Massachusetts Institute of Technology). *Zbtb46*^{DTR} mice were originally characterized by Dr. Nussenzweig (Rockefeller University) and *Batf3*$^{-/-}$ mice were characterized by Dr. Murphy (Washington University School of Medicine). Both *Zbtb46*^{DTR} mice and *Batf3*$^{-/-}$ mice were obtained from Jackson laboratories (JAX:019506; and JAX:013755, respectively) and backcrossed with *Foxp3*$^{GFP\text{-}DTR}$ mice in our laboratory. For diphtheria toxin treatments, mice were injected with 1 µg intraperitoneal (IP) or 250 ng intratumoral (IT) every other day up to three times per week. For syngeneic tumor studies, C57BL/6 mice were subcutaneously inoculated in 100uL of PBS with $5x10^5$ MC38 cells or $5x10^5$ B16F10 cells. For autochthonous tumor studies, sarcomas were induced in *Foxp3*$^{GFP\text{-}DTR}$*;Kras*^{G12D}*;p53*$^{fl/fl}$ mice by intramuscular (IM) injection of the hind calf muscle with replication-incompetent lentiviruses express Cre recombinase as reported previously. Mice were monitored three times per week for palpable sarcoma formation beginning 50 days after IM injection. Tumor measurements were performed blindly using calipers three times per week. A single operator measured each tumor in three dimensions for each tumor measurement. All experiments were performed in accordance with the Institutional Laboratory Animal Care and Use Committee (IACUC) and the Office of Laboratory Animal Care (OLAC) at the University of California, Berkeley.

Lentiviral production

293T cells were transfected with d8.2 (gag/pol), CMV-VSV-G and a transfer vector expressing Cre to produce lentivirus.

Cell lines

MC38 and B16F10 cell lines were kindly provided by Dr. Bluestone (UCSF). All MC38 cell lines expressed luciferase with or without co-expression of mCherry. All cell lines were maintained in DMEM (GIBCO) supplemented with 10% FBS, sodium pyruvate (GIBCO), 10mM HEPES (GIBCO), and penicillin-streptomycin (GIBCO). Tumor cells were grown at 37C with 5% CO_2.

Murine Lymphocyte isolation

Single cell suspensions were generated from lymphoid organs through mechanical disruption of harvested tissues and were passed through 40um filters. Suspensions were resuspended in ice-cold FACS buffer (PBS supplemented with 2mM EDTA and 2% FBS). Spleens were subjected to red blood cell lysis using ACK lysis buffer (150mM NH4Cl, 10mM KHCO3, 0.1mM NA2EDTA, pH 7.3). Resected tumors were minced to 1mm3 isolates and digested in RPMI media supplemented with 4-(2-hydroxyethyl)-1-piperazineethanesulfonic acid (HEPES), 20mg/mL DNase I (Roche), and 125U/mL collagenase D (Roche). Tumor isolates were digested in an orbital shaker for 45 minutes at 37C. All cell suspensions were passed through 40um filters before cell staining or in vitro stimulation. Cytokine staining was performed on 3-5x10^6 cells, after 210 minutes of *in vitro* stimulation in Opti-MEM media supplemented with Brefeldin A (eBioscience), 10ng/mL phorbol 12-myristate 13-acetate (PMA)(Sigma), and 0.25uM ionomycin (Sigma). Fixation and permeabilization of cells was performed for intracellular staining using the Tonbo Foxp3 Transcription Factor Staining Buffer Kit. In some experiments, e.g. staining of APCs for in vivo acquisition of mCherry tumor antigen, cells were fixed with 4% PFA on ice for 15 minutes.

Flow cytometry

Flow cytometry was performed on a BD LSR Fortessa X20 (BD Biosciences) and datasets were analyzed using FlowJo software (Tree Star). All samples analyzed were reconstituted in single cell suspensions using ice-cold FACS buffer (PBS with 2mM EDTA and 2% FBS). Dead cells were stained with Live/Dead Fixable Blue or Aqua Dead Cell Stain kit (Molecular Probes) in PBS for 20 minutes at 4C. Cell surface proteins were stained for 20 minutes at 4C using a mixture of fluorophore-conjugated antibodies. Surface marker stains for murine samples were carried out with anti-mouse CD4 (RM4-5, BioLegend), anti-mouse CD8a (53-6.7, BioLegend), anti-CD25 (PC61, BioLegend), anti-mouse CD44 (IM7, BioLeged), anti-mouse CD45 (30-F11, BioLegend), anti-mouse CD103 (2E7, BioLegend), anti-mouse PD1 (29F.1A12, BioLegend), anti-mouse CCR8 (SA214G2, Biolegend), anti-mouse MHCII (M5/114.15.2, BioLegend), anti-H-2Kb MuLV p15E Tetramer-KSPWFTTL (NIH tetramer core), anti-mouse TIGIT (Vstm3, Biolegend), anti-mouse ICOS (C398.4A, Biolegend), anti-mouse CD62L (MEL1-14, Biolegend) anti-mouse CD11b (M1/70, Biolegend), anti-mouse CD3e (17A2, Biolegend), anti-mouse B220 (FA3-6B2, Biolegend), anti-mouse F4/80 (BM8, Biolegend), anti-mouse CD80 (M16-10A1, Biolegend), anti-mouse CD86 (GL-1, Biolegend) and anti-mouse PD-L1 (10F.9G2, Biolegend). anti-mouse CD11c (N418, Biolegend) in PBS for 20 minutes at 4C. Cells were fixed using the Tonbo Foxp3 Transcription Factor Staining Buffer Kit, prior to intracellular staining. Intracellular staining was performed using anti-mouse anti-mouse Foxp3 (FJK-16S, eBioscience), anti-mouse IL-2 (JES6-5H4, Biolegend), anti-mouse TNF-a (MP6-XT22, BioLegend), anti-mouse IL-10 (JES5-16E3, Biolegend), anti-mouse IFNg (XMG1.2, eBioscience) in PBS for 1 hour at 4C, according to manufacturer's instructions. Cells were resuspended in FACS buffer and filtered through a 40-mm nylon mesh before data acquisition.

In vivo antibody-mediated cell depletion

Immune cell depletion of CD8+ T cells, CD4+ T cells or NK cells was achieved through intraperitoneal injection of 200ug per mouse of each respective depleting antibody. Antibody-based depletion was started at the time of IT DT and was readministered every 6 days throughout the study. CD8b.2 (Clone 53-5.8, Leinco Technologies, Catalog # C2832) was used for CD8+ T cell depletions. Clone GK1.4 (Leinco Technologies, Catalog #C1333) was used for CD4+ T cell depletions. Clone PK136 (Leinco Technologies, Catalog #N123) was used for NK cell depletions. Anti-CCR8 mIgG2a (Gilead Sciences) was administered at 200 ug IP seven days after tumor inoculation and was re-dosed every 3 days.

Bone marrow chimera generation

Host CD45.1+ C57/BL6 mice were administered two doses of 5 Gy irradiation, 16 hours apart. An Xrad320 (Precision X-Ray Irradiation) was used to administer irradiation. 4 hours after the second irradiation treatment, 10x106 bone marrow cells were transferred to host mice via tail vein injection. Bone marrow was harvested from donor *Zbtb46*^{DTR}, *Foxp3*^{DTR}, or *Zbtb46*^{DTR}*Foxp3*^{DTR} CD45.2+ C57/BL6 mice. Femurs and tibias were harvested from euthanized donor mice and flushed with ice-cold RPMI supplemented with 2% FBS, using a 27-gauge syringe. Red blood cells were removed from bone marrow preparations by using ACK lysis buffer (150mM NH4Cl, 10mM KHCO3, 0.1mM NA2EDTA, pH 7.3). Bone marrow was then washed with ice-cold PBS three times prior to tail vein injection. After bone marrow transfer, mice were administered water supplemented with sulfamethoxazole-trimethoprim oral suspension (Ani Pharmaceuticals) for 30 days and were monitored daily. Bone marrow was permitted to reconstitute recipient mice for 60 days. Following reconstitution, $5x10^5$ MC38 tumor cells were subcutaneously inoculated. 7 days after tumor inoculation, mice were administered either IT PBS or a combination of 250 ng IT DT and 80 ng intraperitoneal DT.

Statistical methods

p values were obtained from unpaired two-tailed Student's t tests for all statistical comparisons between two groups, and data were displayed as mean ± SEMs. For multiple comparisons, one-way ANOVA was used. For tumor growth curves, two-way ANOVA was used with Tukey's multiple comparisons test performed at each time point or by multiple regression analysis. Survival analysis was performed using one-way chi-square test or Log-rank (Mantel-Cox) test. p values are denoted in figures by $*p < 0.05$, $**p < 0.01$, and $***p < 0.001$.

Data availability

Values Data supporting the findings of this study are available within the article and supplementary files or from the corresponding authors upon request. Source data are provided with this paper.

References

1. Curiel, T. J. *et al.* Specific recruitment of regulatory T cells in ovarian carcinoma fosters immune privilege and predicts reduced survival. *Nat. Med.* **10**, 942–949 (2004).
2. Fridman, W. H., Pagès, F., Sautès-Fridman, C. & Galon, J. The immune contexture in human tumours: impact on clinical outcome. *Nat. Rev. Cancer* **12**, 298–306 (2012).
3. Jensen, H. K., Donskov, F., Nordsmark, M., Marcussen, N. & von der Maase, H. Increased intratumoral FOXP3-positive regulatory immune cells during interleukin-2 treatment in metastatic renal cell carcinoma. *Clin. Cancer Res.* **15**, 1052–1058 (2009).
4. Sasaki, A. *et al.* Prognostic value of tumor-infiltrating FOXP3+ regulatory T cells in patients with hepatocellular carcinoma. *Eur. J. Surg. Oncol.* **34**, 173–179 (2008).
5. Tao, H. *et al.* Prognostic potential of FOXP3 expression in non-small cell lung cancer cells combined with tumor-infiltrating regulatory T cells. *Lung Cancer* **75**, 95–101 (2012).
6. Shang, B., Liu, Y., Jiang, S.-J. & Liu, Y. Prognostic value of tumor-infiltrating FoxP3+ regulatory T cells in cancers: a systematic review and meta-analysis. *Sci. Rep.* **5**, 15179 (2015).
7. Dikiy, S. & Rudensky, A. Y. Principles of regulatory T cell function. *Immunity* **56**, 240–255 (2023).
8. Togashi, Y., Shitara, K. & Nishikawa, H. Regulatory T cells in cancer immunosuppression - implications for anticancer therapy. *Nat. Rev. Clin. Oncol.* **16**, 356–371 (2019).
9. Tay, C., Tanaka, A. & Sakaguchi, S. Tumor-infiltrating regulatory T cells as targets of cancer immunotherapy. *Cancer Cell* **41**, 450–465 (2023).
10. Shan, F., Somasundaram, A., Bruno, T. C., Workman, C. J. & Vignali, D. A. A. Therapeutic targeting of regulatory T cells in cancer. *Trends Cancer* **8**, 944–961 (2022).

11. Kim, J. M., Rasmussen, J. P. & Rudensky, A. Y. Regulatory T cells prevent catastrophic autoimmunity throughout the lifespan of mice. *Nat. Immunol.* **8**, 191–197 (2007).

12. Bennett, C. L. *et al.* The immune dysregulation, polyendocrinopathy, enteropathy, X-linked syndrome (IPEX) is caused by mutations of FOXP3. *Nat. Genet.* **27**, 20–21 (2001).

13. Sakaguchi, S., Yamaguchi, T., Nomura, T. & Ono, M. Regulatory T cells and immune tolerance. *Cell* **133**, 775–787 (2008).

14. Sakaguchi, S., Sakaguchi, N., Asano, M., Itoh, M. & Toda, M. Immunologic self-tolerance maintained by activated T cells expressing IL-2 receptor alpha-chains (CD25). Breakdown of a single mechanism of self-tolerance causes various autoimmune diseases. *J. Immunol.* **155**, 1151–1164 (1995).

15. Zhou, X. *et al.* Precise spatiotemporal interruption of regulatory T-cell-mediated CD8+ T-cell suppression leads to tumor immunity. *Cancer Res.* **79**, 585–597 (2019).

16. Zagorulya, M. *et al.* Tissue-specific abundance of interferon-gamma drives regulatory T cells to restrain DC1-mediated priming of cytotoxic T cells against lung cancer. *Immunity* **56**, 386–405.e10 (2023).

17. Binnewies, M. *et al.* Unleashing type-2 dendritic cells to drive protective antitumor CD4+ T cell immunity. *Cell* **177**, 556–571.e16 (2019).

18. Deng, L. *et al.* Accumulation of foxp3+ T regulatory cells in draining lymph nodes correlates with disease progression and immune suppression in colorectal cancer patients. *Clin. Cancer Res.* **16**, 4105–4112 (2010).

19. Núñez, N. G. *et al.* Tumor invasion in draining lymph nodes is associated with Treg accumulation in breast cancer patients. *Nat. Commun.* **11**, 3272 (2020).

20. Tanaka, A. & Sakaguchi, S. Targeting Treg cells in cancer immunotherapy. *Eur. J. Immunol.*

49, 1140–1146 (2019).

21. Selby, M. J. *et al.* Anti-CTLA-4 antibodies of IgG2a isotype enhance antitumor activity through reduction of intratumoral regulatory T cells. *Cancer Immunol. Res.* **1**, 32–42 (2013).
22. Simpson, T. R. *et al.* Fc-dependent depletion of tumor-infiltrating regulatory T cells co-defines the efficacy of anti-CTLA-4 therapy against melanoma. *J. Exp. Med.* **210**, 1695–1710 (2013).
23. Liu, C., Workman, C. J. & Vignali, D. A. A. Targeting regulatory T cells in tumors. *FEBS J.* **283**, 2731–2748 (2016).
24. Piconese, S., Valzasina, B. & Colombo, M. P. OX40 triggering blocks suppression by regulatory T cells and facilitates tumor rejection. *J. Exp. Med.* **205**, 825–839 (2008).
25. Sugiyama, D. *et al.* Anti-CCR4 mAb selectively depletes effector-type FoxP3+CD4+ regulatory T cells, evoking antitumor immune responses in humans. *Proc. Natl. Acad. Sci. U. S. A.* **110**, 17945–17950 (2013).
26. Marshall, L. A. *et al.* Tumors establish resistance to immunotherapy by regulating Treg recruitment via CCR4. *J. Immunother. Cancer* **8**, e000764 (2020).
27. Lax, B. M. *et al.* Both intratumoral regulatory T cell depletion and CTLA-4 antagonism are required for maximum efficacy of anti-CTLA-4 antibodies. *Proc. Natl. Acad. Sci. U. S. A.* **120**, e2300895120 (2023).
28. Haruna, M. *et al.* The impact of CCR8+ regulatory T cells on cytotoxic T cell function in human lung cancer. *Sci. Rep.* **12**, 5377 (2022).
29. Whiteside, S. K. *et al.* CCR8 marks highly suppressive Treg cells within tumours but is dispensable for their accumulation and suppressive function. *Immunology* **163**, 512–520

(2021).

30. Soler, D. *et al.* CCR8 expression identifies CD4 memory T cells enriched for FOXP3+ regulatory and Th2 effector lymphocytes. *J. Immunol.* **177**, 6940–6951 (2006).

31. De Simone, M. *et al.* Transcriptional landscape of human tissue lymphocytes unveils uniqueness of tumor-infiltrating T regulatory cells. *Immunity* **45**, 1135–1147 (2016).

32. Plitas, G. *et al.* Regulatory T cells exhibit distinct features in human breast cancer. *Immunity* **45**, 1122–1134 (2016).

33. Villarreal, D. O. *et al.* Targeting CCR8 induces protective antitumor immunity and enhances vaccine-induced responses in colon cancer. *Cancer Res.* **78**, 5340–5348 (2018).

34. Van Damme, H. *et al.* Therapeutic depletion of CCR8+ tumor-infiltrating regulatory T cells elicits antitumor immunity and synergizes with anti-PD-1 therapy. *J. Immunother. Cancer* **9**, e001749 (2021).

35. Campbell, J. R. *et al.* Fc-optimized anti-CCR8 antibody depletes regulatory T cells in human tumor models. *Cancer Res.* **81**, 2983–2994 (2021).

36. Wang, T. *et al.* CCR8 blockade primes anti-tumor immunity through intratumoral regulatory T cells destabilization in muscle-invasive bladder cancer. *Cancer Immunol. Immunother.* **69**, 1855–1867 (2020).

37. Weaver, J. D. *et al.* Differential expression of CCR8 in tumors versus normal tissue allows specific depletion of tumor-infiltrating T regulatory cells by GS-1811, a novel Fc-optimized anti-CCR8 antibody. *Oncoimmunology* **11**, 2141007 (2022).

38. Kidani, Y. *et al.* CCR8-targeted specific depletion of clonally expanded Treg cells in tumor tissues evokes potent tumor immunity with long-lasting memory. *Proc. Natl. Acad. Sci. U. S. A.* **119**, e2114282119 (2022).

39. Jacobs, J. F. M. *et al.* Dendritic cell vaccination in combination with anti-CD25 monoclonal antibody treatment: a phase I/II study in metastatic melanoma patients. *Clin. Cancer Res.* **16**, 5067–5078 (2010).

40. Doi, T. *et al.* A phase I study of the anti-CC chemokine receptor 4 antibody, mogamulizumab, in combination with nivolumab in patients with advanced or metastatic solid tumors. *Clin. Cancer Res.* **25**, 6614–6622 (2019).

41. Sharma, A. *et al.* Anti-CTLA-4 immunotherapy does not deplete FOXP3+ regulatory T cells (tregs) in human cancers. *Clin. Cancer Res.* **25**, 1233–1238 (2019).

42. Bulliard, Y. *et al.* Activating Fc γ receptors contribute to the antitumor activities of immunoregulatory receptor-targeting antibodies. *J. Exp. Med.* **210**, 1685–1693 (2013).

43. Yofe, I. *et al.* Anti-CTLA-4 antibodies drive myeloid activation and reprogram the tumor microenvironment through FcγR engagement and type I interferon signaling. *Nat. Cancer* **3**, 1336–1350 (2022).

44. Dahan, R. *et al.* Therapeutic activity of agonistic, human anti-CD40 monoclonal antibodies requires selective FcγR engagement. *Cancer Cell* **29**, 820–831 (2016).

45. Miller, C. L. *et al.* Targeted TLR9 agonist elicits effective antitumor immunity against spontaneously arising breast tumors. *J. Immunol.* **211**, 295–305 (2023).

46. Hong, W. X., Sagiv-Barfi, I., Czerwinski, D. K., Sallets, A. & Levy, R. Neoadjuvant intratumoral immunotherapy with TLR9 activation and anti-OX40 antibody eradicates metastatic cancer. *Cancer Res.* **82**, 1396–1408 (2022).

47. Marabelle, A. *et al.* Depleting tumor-specific Tregs at a single site eradicates disseminated tumors. *J. Clin. Invest.* **123**, 2447–2463 (2013).

48. Sagiv-Barfi, I., Czerwinski, D. K., Shree, T., Lohmeyer, J. J. K. & Levy, R. Intratumoral

immunotherapy relies on B and T cell collaboration. *Sci. Immunol.* **7**, eabn5859 (2022).

49. Hong, W. X. *et al.* Intratumoral immunotherapy for early-stage solid tumors. *Clin. Cancer Res.* **26**, 3091–3099 (2020).
50. Guan, X. *et al.* Anti-TIGIT antibody improves PD-L1 blockade through myeloid and Treg cells. *Nature* **627**, 646–655 (2024).
51. Bos, P. D., Plitas, G., Rudra, D., Lee, S. Y. & Rudensky, A. Y. Transient regulatory T cell ablation deters oncogene-driven breast cancer and enhances radiotherapy. *J. Exp. Med.* **210**, 2435–2466 (2013).
52. Pastille, E. *et al.* Transient ablation of regulatory T cells improves antitumor immunity in colitis-associated colon cancer. *Cancer Res.* **74**, 4258–4269 (2014).
53. Teng, M. W. L. *et al.* Multiple antitumor mechanisms downstream of prophylactic regulatory T-cell depletion. *Cancer Res.* **70**, 2665–2674 (2010).
54. Shimizu, J., Yamazaki, S. & Sakaguchi, S. Induction of tumor immunity by removing CD25+CD4+ T cells: a common basis between tumor immunity and autoimmunity. *J. Immunol.* **163**, 5211–5218 (1999).
55. Piersiala, K. *et al.* Tumour-draining lymph nodes in head and neck cancer are characterized by accumulation of CTLA-4 and PD-1 expressing Treg cells. *Transl. Oncol.* **23**, 101469 (2022).
56. Kirsch, D. G. *et al.* A spatially and temporally restricted mouse model of soft tissue sarcoma. *Nat. Med.* **13**, 992–997 (2007).
57. DuPage, M., Mazumdar, C., Schmidt, L. M., Cheung, A. F. & Jacks, T. Expression of tumour-specific antigens underlies cancer immunoediting. *Nature* **482**, 405–409 (2012).
58. DuPage, M. *et al.* Endogenous T cell responses to antigens expressed in lung

adenocarcinomas delay malignant tumor progression. *Cancer Cell* **19**, 72–85 (2011).

59. Joshi, N. S. *et al.* Regulatory T cells in tumor-associated tertiary lymphoid structures suppress anti-tumor T cell responses. *Immunity* **43**, 579–590 (2015).
60. Fransen, M. F., van der Sluis, T. C., Ossendorp, F., Arens, R. & Melief, C. J. M. Controlled local delivery of CTLA-4 blocking antibody induces CD8+ T-cell-dependent tumor eradication and decreases risk of toxic side effects. *Clin. Cancer Res.* **19**, 5381–5389 (2013).
61. Geels, S. N. *et al.* Interruption of the intratumor CD8+ T cell:Treg crosstalk improves the efficacy of PD-1 immunotherapy. *Cancer Cell* **42**, 1051–1066.e7 (2024).
62. Takahashi, M. *et al.* Intratumoral antigen signaling traps CD8+ T cells to confine exhaustion to the tumor site. *Sci. Immunol.* **9**, eade2094 (2024).
63. Zhou, L. *et al.* Spatial and functional targeting of intratumoral Tregs reverses CD8+ T cell exhaustion and promotes cancer immunotherapy. *J. Clin. Invest.* **134**, (2024).
64. Meredith, M. M. *et al.* Expression of the zinc finger transcription factor zDC (Zbtb46, Btbd4) defines the classical dendritic cell lineage. *J. Exp. Med.* **209**, 1153–1165 (2012).
65. Satpathy, A. T. *et al.* Zbtb46 expression distinguishes classical dendritic cells and their committed progenitors from other immune lineages. *J. Exp. Med.* **209**, 1135–1152 (2012).
66. Zagorulya, M. & Spranger, S. Once upon a prime: DCs shape cancer immunity. *Trends Cancer* **9**, 172–184 (2023).
67. Moreno Ayala, M. A. *et al.* CXCR3 expression in regulatory T cells drives interactions with type I dendritic cells in tumors to restrict CD8+ T cell antitumor immunity. *Immunity* **56**, 1613–1630.e5 (2023).
68. Pittet, M. J., Di Pilato, M., Garris, C. & Mempel, T. R. Dendritic cells as shepherds of T cell

immunity in cancer. *Immunity* **56**, 2218–2230 (2023).

69. Yin, X., Chen, S. & Eisenbarth, S. C. Dendritic cell regulation of T helper cells. *Annu. Rev. Immunol.* **39**, 759–790 (2021).
70. Qureshi, O. S. *et al.* Trans-endocytosis of CD80 and CD86: a molecular basis for the cell-extrinsic function of CTLA-4. *Science* **332**, 600–603 (2011).
71. Wing, K. *et al.* CTLA-4 control over Foxp3+ regulatory T cell function. *Science* **322**, 271–275 (2008).
72. He, X. & Xu, C. Immune checkpoint signaling and cancer immunotherapy. *Cell Res.* **30**, 660–669 (2020).
73. Overacre-Delgoffe, A. E. *et al.* Interferon-γ drives Treg fragility to promote anti-tumor immunity. *Cell* **169**, 1130–1141.e11 (2017).
74. Spranger, S., Dai, D., Horton, B. & Gajewski, T. F. Tumor-residing Batf3 dendritic cells are required for effector T cell trafficking and adoptive T cell therapy. *Cancer Cell* **31**, 711–723.e4 (2017).
75. Broz, M. L. *et al.* Dissecting the tumor myeloid compartment reveals rare activating antigen-presenting cells critical for T cell immunity. *Cancer Cell* **26**, 938 (2014).
76. Hildner, K. *et al.* Batf3 deficiency reveals a critical role for CD8alpha+ dendritic cells in cytotoxic T cell immunity. *Science* **322**, 1097–1100 (2008).
77. Salmon, H. *et al.* Expansion and activation of CD103(+) dendritic cell progenitors at the tumor site enhances tumor responses to therapeutic PD-L1 and BRAF inhibition. *Immunity* **44**, 924–938 (2016).
78. Maier, B. *et al.* A conserved dendritic-cell regulatory program limits antitumour immunity. *Nature* **580**, 257–262 (2020).

79. You, S. *et al.* Lymphatic-localized Treg-mregDC crosstalk limits antigen trafficking and restrains anti-tumor immunity. *Cancer Cell* **42**, 1415–1433.e12 (2024).

80. Xiao, L. *et al.* Adoptively transferred tumor-specific IL-9-producing cytotoxic CD8+ T cells activate host CD4+ T cells to control tumors with antigen loss. *Nat. Cancer* **6**, 718–735 (2025).

81. Ho, W. W. *et al.* Dendritic cell paucity in mismatch repair-proficient colorectal cancer liver metastases limits immune checkpoint blockade efficacy. *Proc. Natl. Acad. Sci. U. S. A.* **118**, e2105323118 (2021).

82. Budhu, A. *et al.* Tumor biology and immune infiltration define primary liver cancer subsets linked to overall survival after immunotherapy. *Cell Rep. Med.* **4**, 101052 (2023).

83. Hegde, S. *et al.* Dendritic cell paucity leads to dysfunctional immune surveillance in pancreatic cancer. *Cancer Cell* **37**, 289–307.e9 (2020).

84. Hashimoto, M., Ramalingam, S. S. & Ahmed, R. Harnessing CD8 T cell responses using PD-1-IL-2 combination therapy. *Trends Cancer* **10**, 332–346 (2024).

85. Taylor, B. C. & Balko, J. M. Mechanisms of MHC-I downregulation and role in immunotherapy response. *Front. Immunol.* **13**, 844866 (2022).

86. Schumacher, T. N. & Schreiber, R. D. Neoantigens in cancer immunotherapy. *Science* **348**, 69–74 (2015).

87. MacNabb, B. W. *et al.* Dendritic cells can prime anti-tumor CD8+ T cell responses through major histocompatibility complex cross-dressing. *Immunity* **55**, 2206–2208 (2022).

88. McGranahan, N. *et al.* Allele-specific HLA loss and immune escape in lung cancer evolution. *Cell* **171**, 1259–1271.e11 (2017).

Acknowledgements

We thank David Raulet, Ellen Robey, Greg Barton and members of the DuPage laboratory for reviewing the manuscript and providing feedback. We also thank Hector Nolla, Alma Valleros, Kartoosh Heydari, Melaine Delcroix and Harman Dhaliwal of the UC Berkeley Cancer Research Laboratory Flow Cytometry Facility. Furthermore, we thank all the members of the DuPage lab for providing guidance on the research approach. M.D is a Pew-Stewart Scholar and a St. Baldrick's Scholar with generous support from Hope with Hazel.

Author Contributions

Conceptualization and methodology, M.D. and A.B.; Investigation, A.B., B.G. and M.D.; writing - original draft, M.D. and A.B; writing - review & editing, M.D., A.B., B.G., C.Z.; supervision, M.D. and A.B.; funding acquisition, M.D.

Competing Interests

M.D. is supported by Gilead Sciences, which provided funding and anti-CCR8 antibody reagents that supported this work. The other authors declare no competing interests.

Additional information

Correspondence and requests for materials should be addressed to Alissa Bockman or Michel DuPage.

FIGURE 1

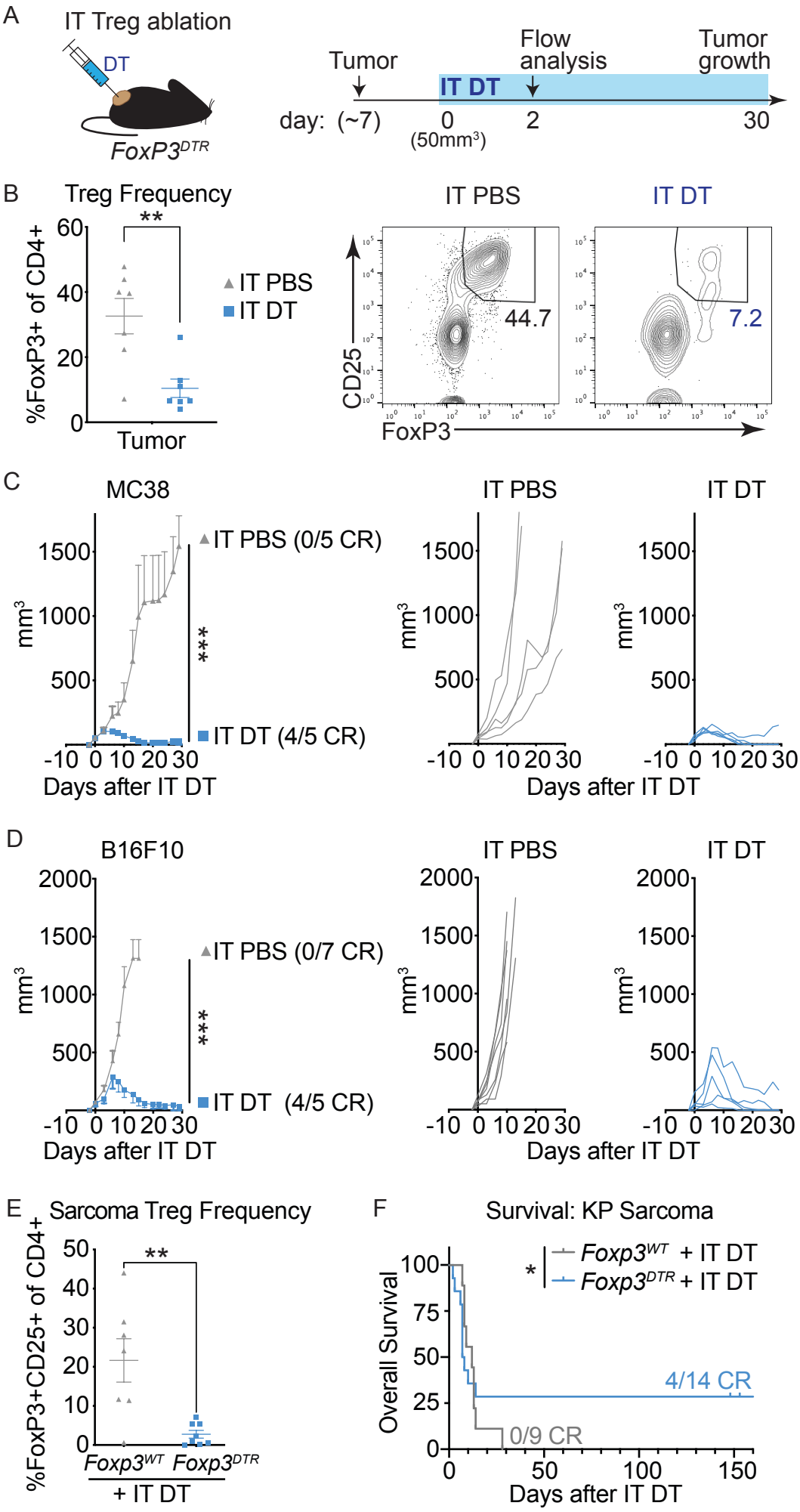
A
IT Treg ablation
DT
FoxP3DTR
Tumor
Flow analysis
Tumor growth
IT DT
day: (~7)
0
(50mm3)
2
30
B
Treg Frequency
%FoxP3+ of CD4+
IT PBS
IT DT
Tumor
IT PBS
IT DT
44.7
7.2
CD25
FoxP3
C
MC38
IT PBS (0/5 CR)
IT DT (4/5 CR)
mm3
Days after IT DT
IT PBS
IT DT
D
B16F10
IT PBS (0/7 CR)
IT DT (4/5 CR)
mm3
Days after IT DT
IT PBS
IT DT
E
Sarcoma Treg Frequency
%FoxP3+CD25+ of CD4+
Foxp3WT
Foxp3DTR
+ IT DT
F
Survival: KP Sarcoma
Foxp3WT + IT DT
Foxp3DTR + IT DT
Overall Survival
4/14 CR
0/9 CR
Days after IT DT

Figure 1. Intratumoral Treg depletion is sufficient to control tumor growth.
(A) Experimental design for intratumoral diphtheria toxin (IT DT) injection in *Foxp3*^{DTR} mice. DT was administered every 48-72 hours beginning when tumors were 50mm^3 and throughout the study.
(B) IT Treg frequencies in MC38 tumor-bearing *Foxp3*^{DTR} mice 48 hours after one dose of IT PBS or IT DT. Representative flow cytometric staining for FoxP3+ CD25+ Tregs of live CD4+ T cells.
(C-D) MC38 tumor growth (C) or B16F10 tumor growth (D) in *Foxp3*^{DTR} mice after sustained IT DT or IT PBS treatment. Data are representative of 4-10 independent experiments for each tumor type.
(E) IT Treg frequencies in IT DT treated *K-ras*^{G12D}*;p53*$^{-/-}$ versus *Foxp3*$^{DTR\text{-}GFP}$*;K-ras*^{G12D}*;p53*$^{-/-}$ autochthonous sarcomas.
(F) Survival analysis of sarcoma-bearing mice after IT DT treatment beginning when palpable mass was detected.
Data represent means ± SEM; *$p < 0.05$, **$p < 0.01$ and ***$p < 0.001$. B,E: Unpaired two-tailed T test. C,D: Ordinary two-way ANOVA with Tukey's multiple comparison test. F: One-sided Chi-square test. (n=5-14 mice/group).

FIGURE 2

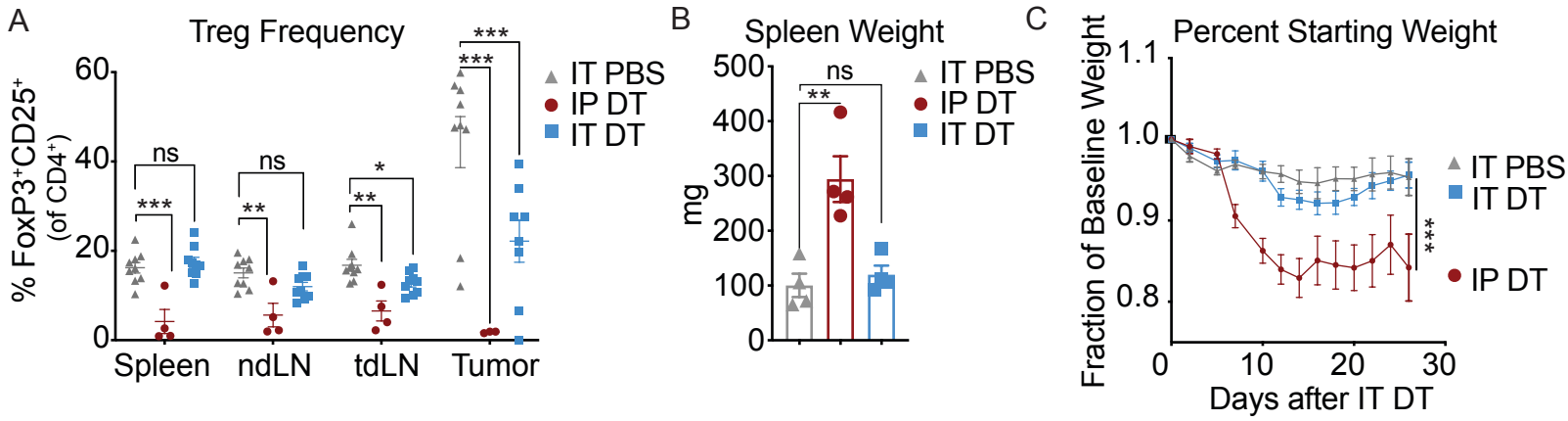

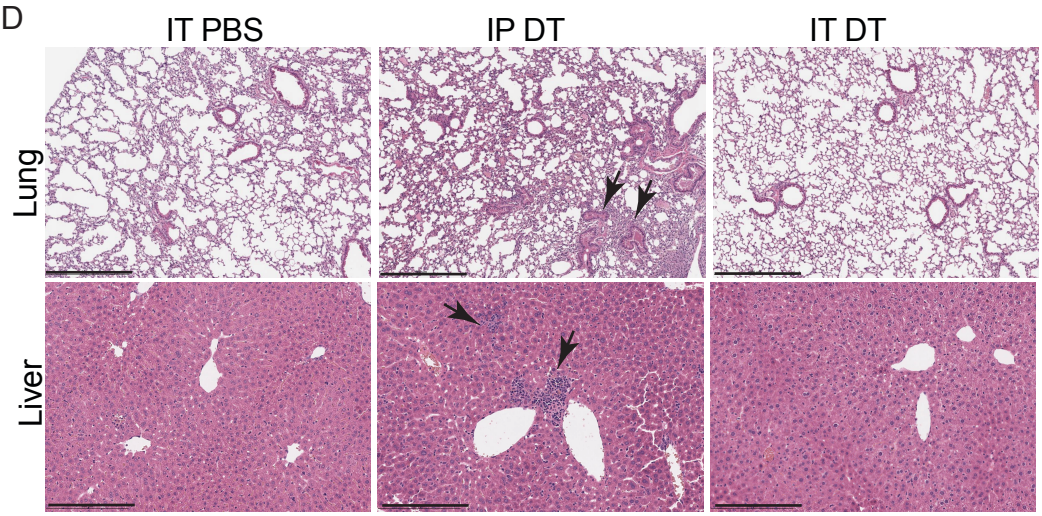

E

Pathology score: severely damaged (++), damaged (+), normal (-)

Group	Sample ID	Lung	Liver	Treatment
1	494	+	-	IT PBS
	495	+	-	
2	238	+	+	IP DT
	386	++	+	
3	239	-	-	IT DT
	385	-	-	

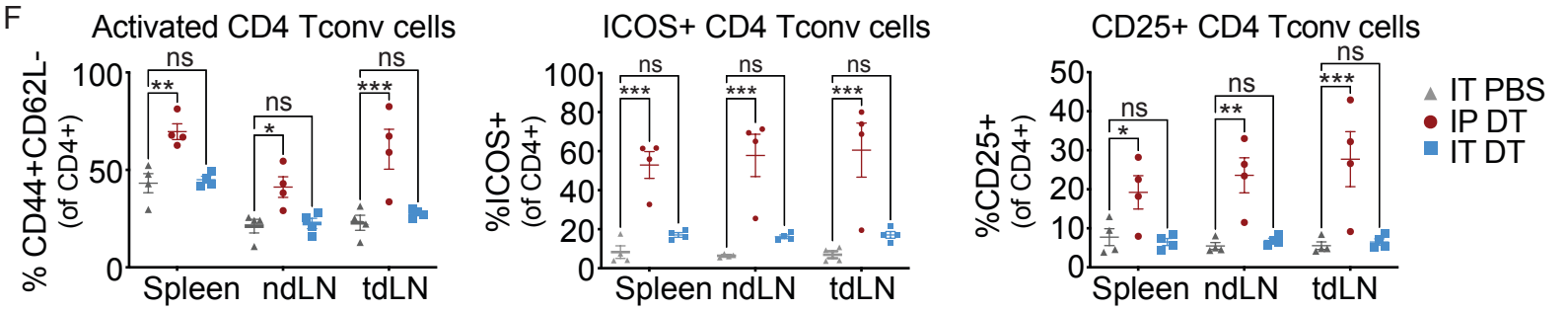

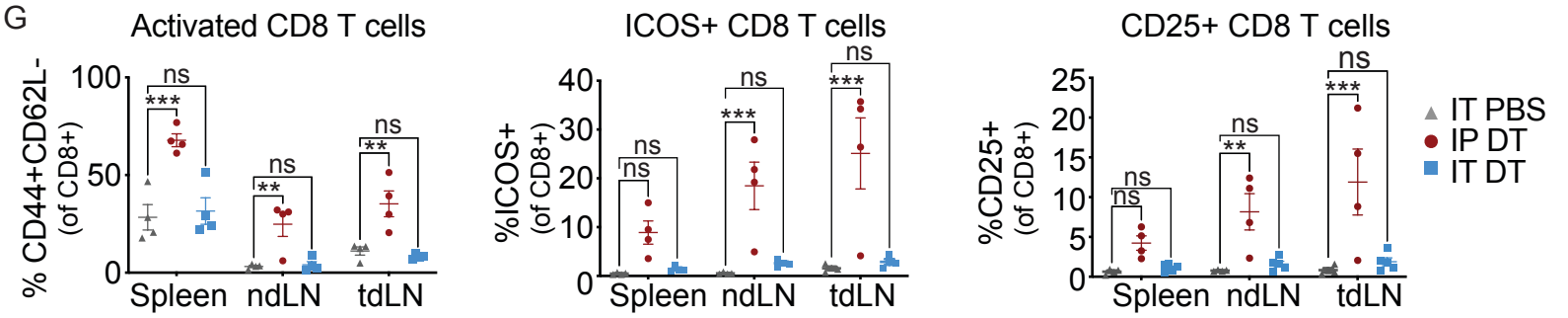

Figure 2. IT Treg ablation, unlike systemic Treg ablation, does not cause autoimmune pathology.

(A) Treg frequencies in spleen, non-tumor-draining lymph nodes (ndLN), tumor-draining LN (tdLN), and tumor after IP PBS, IP DT, or IT DT in MC38-tumor bearing *Foxp3*^{DTR} mice.

(B) Spleen weight in MC38-tumor bearing *Foxp3*^{DTR} mice after 30 days of sustained IP or IT DT treatment.

(C) Body weight of MC38-tumor bearing *Foxp3*^{DTR} mice treated with IP PBS, IP DT, or IT DT.

(D) Hematoxylin and eosin staining performed on lung and liver tissues harvested after sustained IP PBS, IP DT, or IT DT. Arrows indicate lymphocytic infiltrates within tissues. Images are representative of two biological replicates for each treatment group.

(E) Pathology scores of IT PBS, IP DT or IT DT treated mice.

(F-G) Percent of CD4+ (F) and CD8+ (G) T cells expressing CD44, ICOS, and CD25 activation markers after sustained IP PBS, IP DT, or IT DT.

Data are representative of 3 independent experiments. Data represent means ± SEM; *$p < 0.05$, **$p < 0.01$ and ***$p < 0.001$. A,B: Unpaired two-tailed T test. C;F;G: Ordinary two-way ANOVA with Tukey's multiple comparison test. (n=4-9 mice/group).

FIGURE 3

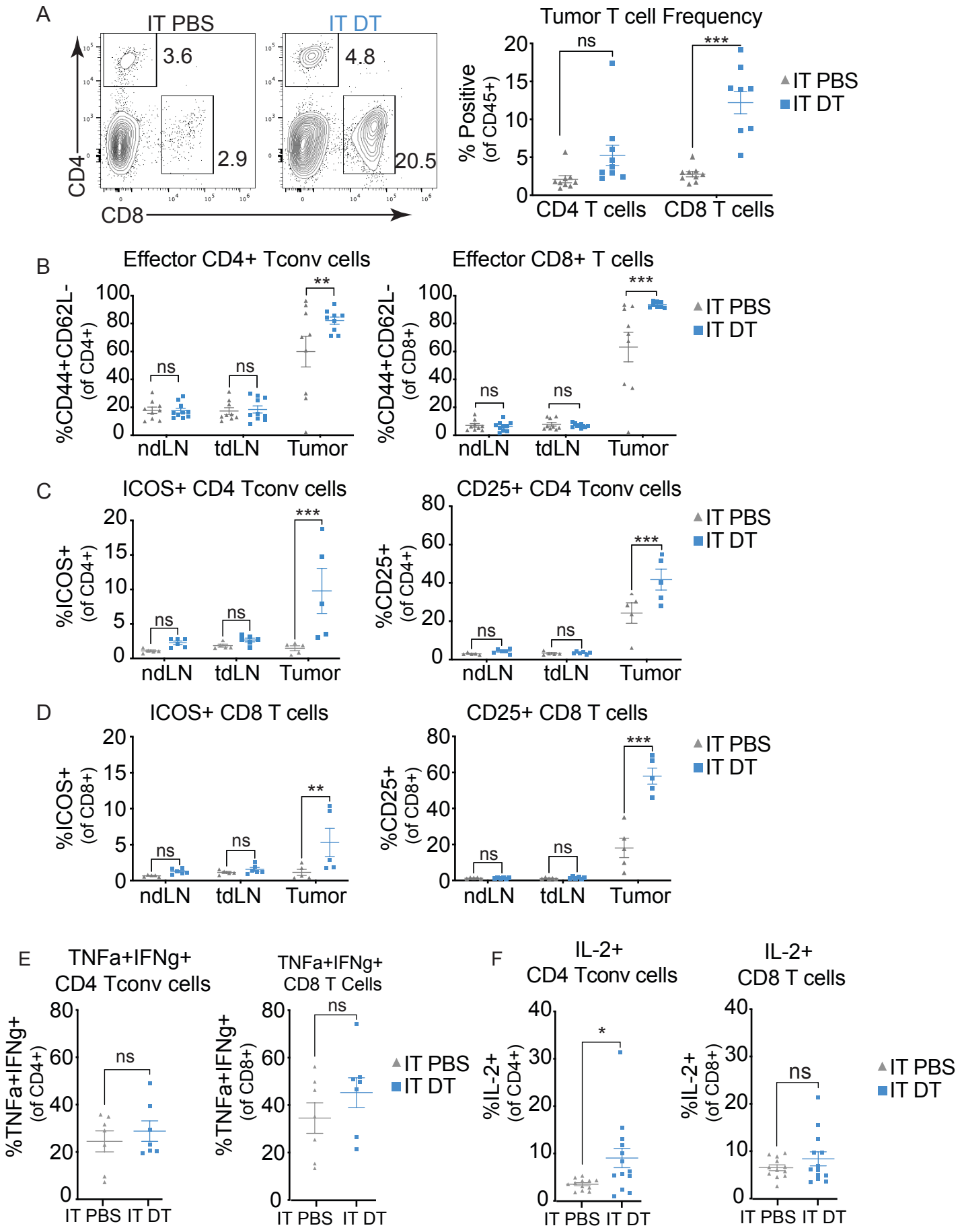
A
IT PBS
IT DT
3.6
2.9
4.8
20.5
CD4
CD8
Tumor T cell Frequency
% Positive (of CD45+)
ns
***
CD4 T cells
CD8 T cells
IT PBS
IT DT
B
Effector CD4+ Tconv cells
Effector CD8+ T cells
%CD44+CD62L- (of CD4+)
%CD44+CD62L- (of CD8+)
**
***
ns
ndLN
tdLN
Tumor
C
ICOS+ CD4 Tconv cells
CD25+ CD4 Tconv cells
%ICOS+ (of CD4+)
%CD25+ (of CD4+)
D
ICOS+ CD8 T cells
CD25+ CD8 T cells
%ICOS+ (of CD8+)
%CD25+ (of CD8+)
E
TNFa+IFNg+ CD4 Tconv cells
TNFa+IFNg+ CD8 T Cells
%TNFa+IFNg+ (of CD4+)
%TNFa+IFNg+ (of CD8+)
F
IL-2+ CD4 Tconv cells
IL-2+ CD8 T cells
%IL-2+ (of CD4+)
%IL-2+ (of CD8+)
*

Figure 3. IT Treg depletion promotes CD8 and CD4 T cell activation locally in tumors.
(A) Representative flow plots and quantification of CD4+ Tconv and CD8+ T cell frequencies in MC38 tumor tissue after sustained PBS or IT DT treatment.
(B) Frequencies of effector (CD44+CD62L-) CD4+ Tconv cell or CD8+ T cells after IT PBS or IT DT.
(C-D)Percentages of CD44+, ICOS+ or CD25+ on CD4+ Tconv cells or (D) CD8+ T cells.
(E) TNFα and IFNγ cytokine expression in tumor-infiltrating CD8+ and CD4+ Tconv cells.
(F) IL-2 cytokine expression in CD4+ Tconv or CD8 T cells after PBS or IT DT treatment.
Data are representative of 2 independent experiments. Data represent means ± SEM; *$p < 0.05$, **$p < 0.01$ and ***$p < 0.001$. A: Unpaired two-tailed T test. B-F: Ordinary two-way ANOVA with Tukey's multiple comparison test. (n=5-10 mice/group).

FIGURE 4

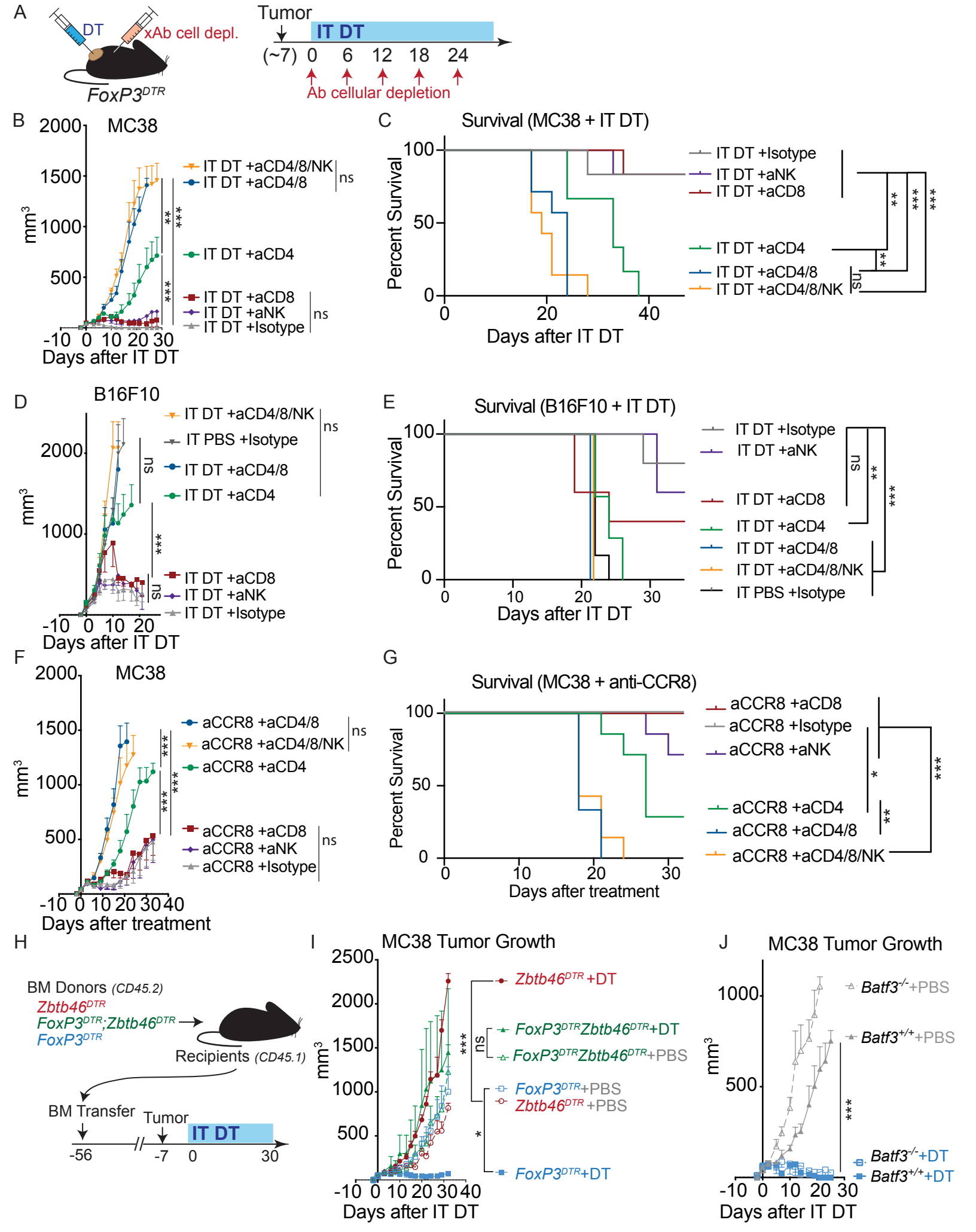
A
DT
xAb cell depl.
FoxP3DTR
Tumor
IT DT
(~7) 0 6 12 18 24
Ab cellular depletion
B
MC38
mm3
IT DT +aCD4/8/NK
IT DT +aCD4/8
IT DT +aCD4
IT DT +aCD8
IT DT +aNK
IT DT +Isotype
ns
Days after IT DT
C
Survival (MC38 + IT DT)
Percent Survival
IT DT +Isotype
IT DT +aNK
IT DT +aCD8
IT DT +aCD4
IT DT +aCD4/8
IT DT +aCD4/8/NK
Days after IT DT
D
B16F10
IT DT +aCD4/8/NK
IT PBS +Isotype
IT DT +aCD4/8
IT DT +aCD4
IT DT +aCD8
IT DT +aNK
IT DT +Isotype
Days after IT DT
E
Survival (B16F10 + IT DT)
IT DT +Isotype
IT DT +aNK
IT DT +aCD8
IT DT +aCD4
IT DT +aCD4/8
IT DT +aCD4/8/NK
IT PBS +Isotype
Days after IT DT
F
MC38
aCCR8 +aCD4/8
aCCR8 +aCD4/8/NK
aCCR8 +aCD4
aCCR8 +aCD8
aCCR8 +aNK
aCCR8 +Isotype
Days after treatment
G
Survival (MC38 + anti-CCR8)
aCCR8 +aCD8
aCCR8 +Isotype
aCCR8 +aNK
aCCR8 +aCD4
aCCR8 +aCD4/8
aCCR8 +aCD4/8/NK
Days after treatment
H
BM Donors (CD45.2)
Zbtb46DTR
FoxP3DTR;Zbtb46DTR
FoxP3DTR
Recipients (CD45.1)
BM Transfer
Tumor
IT DT
-56 -7 0 30
I
MC38 Tumor Growth
Zbtb46DTR +DT
FoxP3DTRZbtb46DTR+DT
FoxP3DTRZbtb46DTR+PBS
FoxP3DTR+PBS
Zbtb46DTR +PBS
FoxP3DTR+DT
Days after IT DT
J
MC38 Tumor Growth
Batf3-/-+PBS
Batf3+/++PBS
Batf3-/-+DT
Batf3+/++DT
Days after IT DT

Figure 4. Conventional CD4+ T cells control tumors after IT Treg ablation.
(A) Experimental design for cellular depletion studies in *Foxp3*^{DTR} mice. IT Treg ablation was achieved through either IT DT or anti-CCR8 and began concurrent with cellular depletion. *In vivo* depletion antibodies were administered IP every 6 days for the duration of the study.
(B) MC38 tumor growth in *Foxp3*^{DTR} mice that received IT DT and indicated cellular depleting antibodies.
(C)Animal survival after IT DT treatment and indicated cellular depletion. One experiment performed.
(D) B16F10 tumor growth in *Foxp3*^{DTR} mice that received IT DT and indicated cellular depleting antibodies.
(E) Animal survival after IT DT and indicated cellular depletion. One experiment performed.
(F) MC38 tumor growth after anti-CCR8 treatment and indicated cellular depletion.
(G) Animal survival after anti-CCR8 and cellular depletion. One experiment performed.
(H) Schematic of bone marrow chimera generation and treatment regimen in *Zbtb46*^{DTR}*Foxp3*^{DTR} chimeric mice. 250 ng IT DT and 80 ng IP DT was administered every 48-72 hours, once MC38 tumors reached 50mm^3.
(I) MC38 tumor growth in *Zbtb46*^{DTR}*Foxp3*^{DTR} chimeric mice. One experiment performed.
(J) MC38 tumor growth in *Foxp3*^{DTR}*Batf3*$^{-/-}$ mice. 250 ng IT DT was administered every 48-72 hours. Data are representative of 3 independent experiments.
Data represent means ± SEM; *$p < 0.05$, **$p < 0.01$ and ***$p < 0.001$. B,D,F; I-J: Ordinary two-way ANOVA with Tukey's multiple comparison test. C,E,J: Log-rank (Mantel-Cox) test. (n=5-7 mice/group).

FIGURE 5

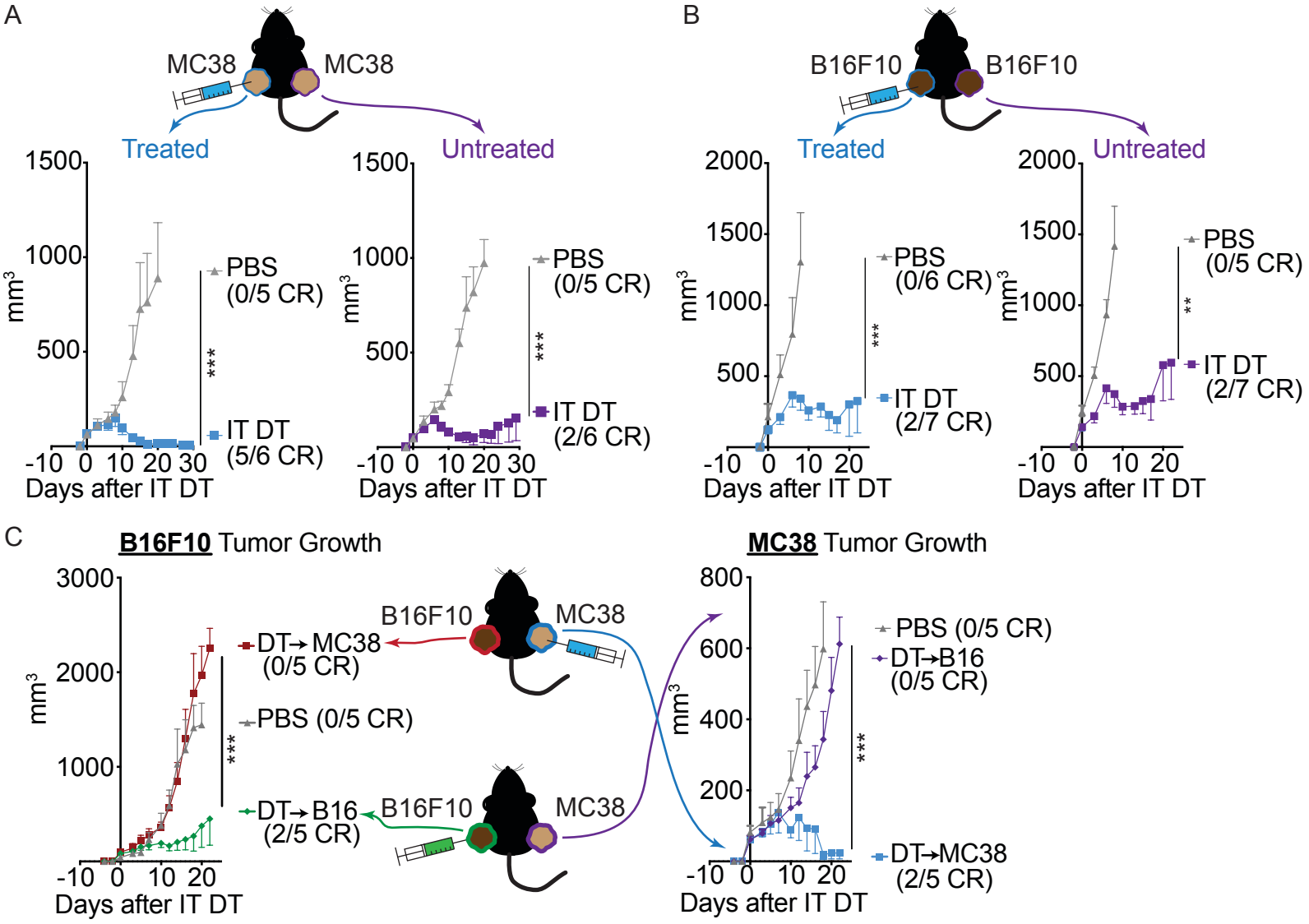
A
MC38
MC38
Treated
Untreated
1500
1000
500
mm3
PBS (0/5 CR)
IT DT (5/6 CR)
***
-10 0 10 20 30
Days after IT DT
PBS (0/5 CR)
IT DT (2/6 CR)
B
B16F10
B16F10
2000
1500
1000
500
PBS (0/6 CR)
IT DT (2/7 CR)
PBS (0/5 CR)
IT DT (2/7 CR)
**
-10 0 10 20
C
B16F10 Tumor Growth
MC38 Tumor Growth
3000
2000
1000
DT→MC38 (0/5 CR)
PBS (0/5 CR)
DT→B16 (2/5 CR)
B16F10
MC38
800
600
400
200
PBS (0/5 CR)
DT→B16 (0/5 CR)
DT→MC38 (2/5 CR)

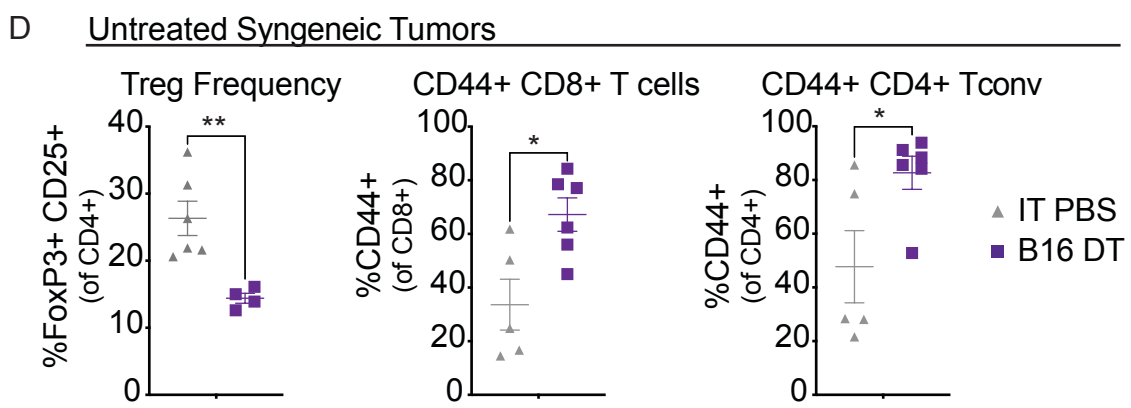
D
Untreated Syngeneic Tumors
Treg Frequency
CD44+ CD8+ T cells
CD44+ CD4+ Tconv
%FoxP3+ CD25+ (of CD4+)
%CD44+ (of CD8+)
%CD44+ (of CD4+)
40
30
20
10
0
100
80
60
40
20
0
**
*
IT PBS
B16 DT

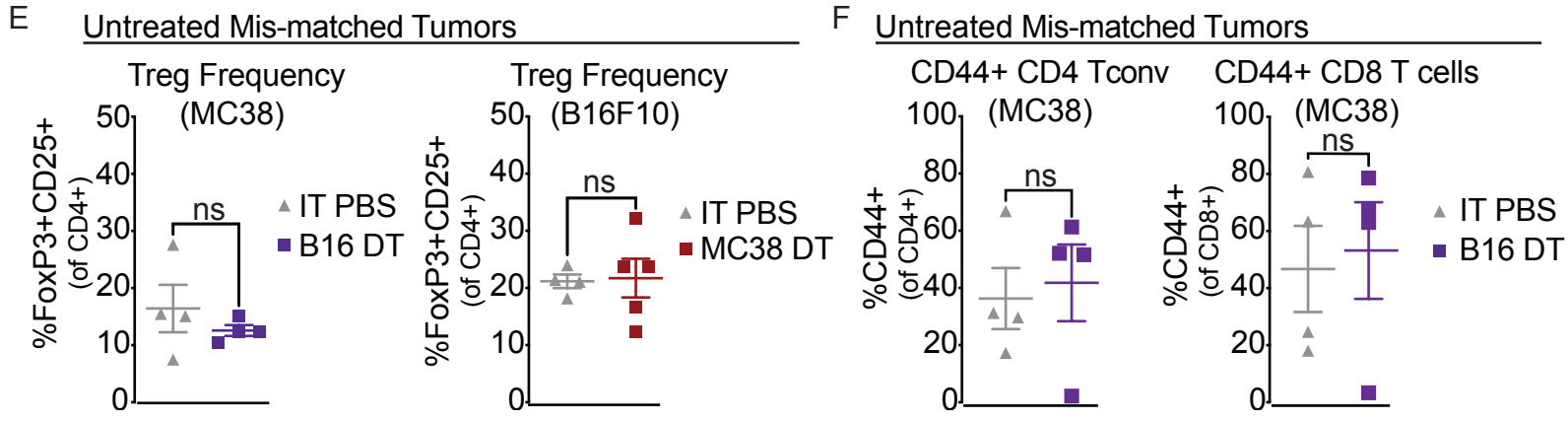
E
Untreated Mis-matched Tumors
Treg Frequency (MC38)
Treg Frequency (B16F10)
%FoxP3+CD25+ (of CD4+)
50
40
30
20
10
0
ns
IT PBS
B16 DT
MC38 DT
F
Untreated Mis-matched Tumors
CD44+ CD4 Tconv (MC38)
CD44+ CD8 T cells (MC38)
%CD44+ (of CD4+)
%CD44+ (of CD8+)
100
80
60
40
20
0

Figure 5. Ablation of IT Tregs in a single tumor unleashes antitumor immunity against syngeneic distal tumors.

(A) MC38 tumor growth of an IT DT treated tumor and a distal, MC38 untreated tumor.
(B) B16F10 tumor growth of an IT DT treated tumor and a distal, untreated B16F10 tumor.
(C) B16F10 or MC38 tumor growth in *Foxp3*^{DTR} mice bearing an MC38 tumor on the right flank and a B16F10 tumor on the left flank. B16F10 tumors are directly treated (green) or MC38 tumors are directly treated (blue). Data are representative of 5 independent experiments.
(D) Quantification of Treg and activated CD4+ Tconv cell and CD8+ T cell frequencies in matched B16F10-tumor bearing mice. Tissue harvest performed at humane experimental endpoint for each cohort (D10 for PBS treated mice and D20 for IT DT treated mice).
(E-F) Quantification of Treg frequencies or (F) activated CD4+ Tconv cells and CD8+ T cells in untreated MC38 or B16F10 tumors after IT DT in a mismatched B16F10 or MC38 tumor, respectively. Tissue harvest performed at humane experimental endpoint for each cohort (D20 for IT DT and IT PBS treated mice).
Data are representative of 5 independent experiments for matched MC38 tumors and 2 independent experiments for matched B16F10 tumors. Data represent means ± SEM; *$p < 0.05$, **$p < 0.01$ and ***$p < 0.001$. A-C: Ordinary two-way ANOVA with Tukey's multiple comparison test. D-F: Unpaired two-tailed T test. (n=4-7 mice/group).

FIGURE 6

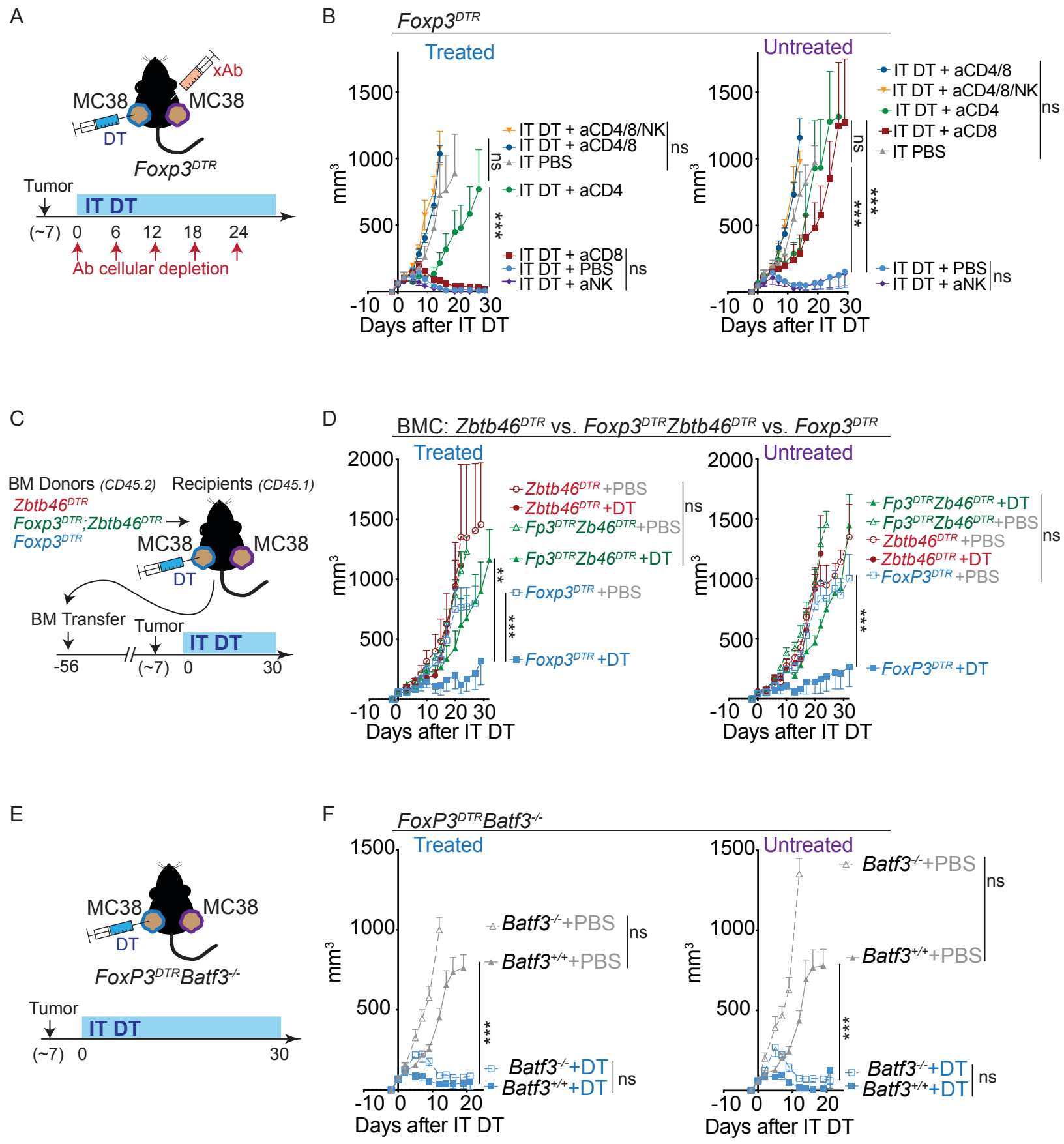
A
xAb
MC38
MC38
DT
Foxp3DTR
Tumor
IT DT
(~7) 0 6 12 18 24
Ab cellular depletion
B
Foxp3DTR
Treated
Untreated
mm3
Days after IT DT
IT DT + aCD4/8/NK
IT DT + aCD4/8
IT PBS
IT DT + aCD4
IT DT + aCD8
IT DT + PBS
IT DT + aNK
ns
***
C
BM Donors (CD45.2)
Recipients (CD45.1)
Zbtb46DTR
Foxp3DTR;Zbtb46DTR
Foxp3DTR
MC38
MC38
DT
BM Transfer
Tumor
IT DT
-56
(~7) 0
30
D
BMC: Zbtb46DTR vs. Foxp3DTRZbtb46DTR vs. Foxp3DTR
Treated
Untreated
Zbtb46DTR +PBS
Zbtb46DTR +DT
Fp3DTRZb46DTR+PBS
Fp3DTRZb46DTR +DT
Foxp3DTR +PBS
Foxp3DTR +DT
FoxP3DTR +PBS
FoxP3DTR +DT
**
E
MC38
MC38
DT
FoxP3DTRBatf3-/-
Tumor
IT DT
(~7) 0
30
F
FoxP3DTRBatf3-/-
Treated
Untreated
Batf3-/-+PBS
Batf3+/+PBS
Batf3-/-+DT
Batf3+/+DT

Figure 6. Control of disseminated tumors is reversed by CD8+ or CD4+ T cell depletions.
(A) Schematic of tumor inoculation and cellular depletion regimen in *Foxp3*^{DTR} mice.
(B) MC38 tumor growth of an IT DT treated tumor or distal, untreated tumor.
(C) Experimental schematic of *Zbtb46*^{DTR}*Foxp3*^{DTR} bone marrow chimera generation.
(D) MC38 tumor growth in *Zbtb46*^{DTR}*Foxp3*^{DTR} bone marrow chimeric mice. One experiment performed.
(E) Experimental setup of IT Treg depletion in *Foxp3*^{DTR}*Batf3*$^{-/-}$ mice.
(F) MC38 tumor growth in an IT DT treated tumor or a distal, untreated tumor in *Foxp3*^{DTR}*Batf3*$^{-/-}$ mice. One experiment performed.
Data are representative of 2-5 independent experiments. Data represent means ± SEM; *$p < 0.05$, **$p < 0.01$ and ***$p < 0.001$. B-G: Ordinary two-way ANOVA with Tukey's multiple comparison test. (n=4-7 mice/group).

FIGURE 7

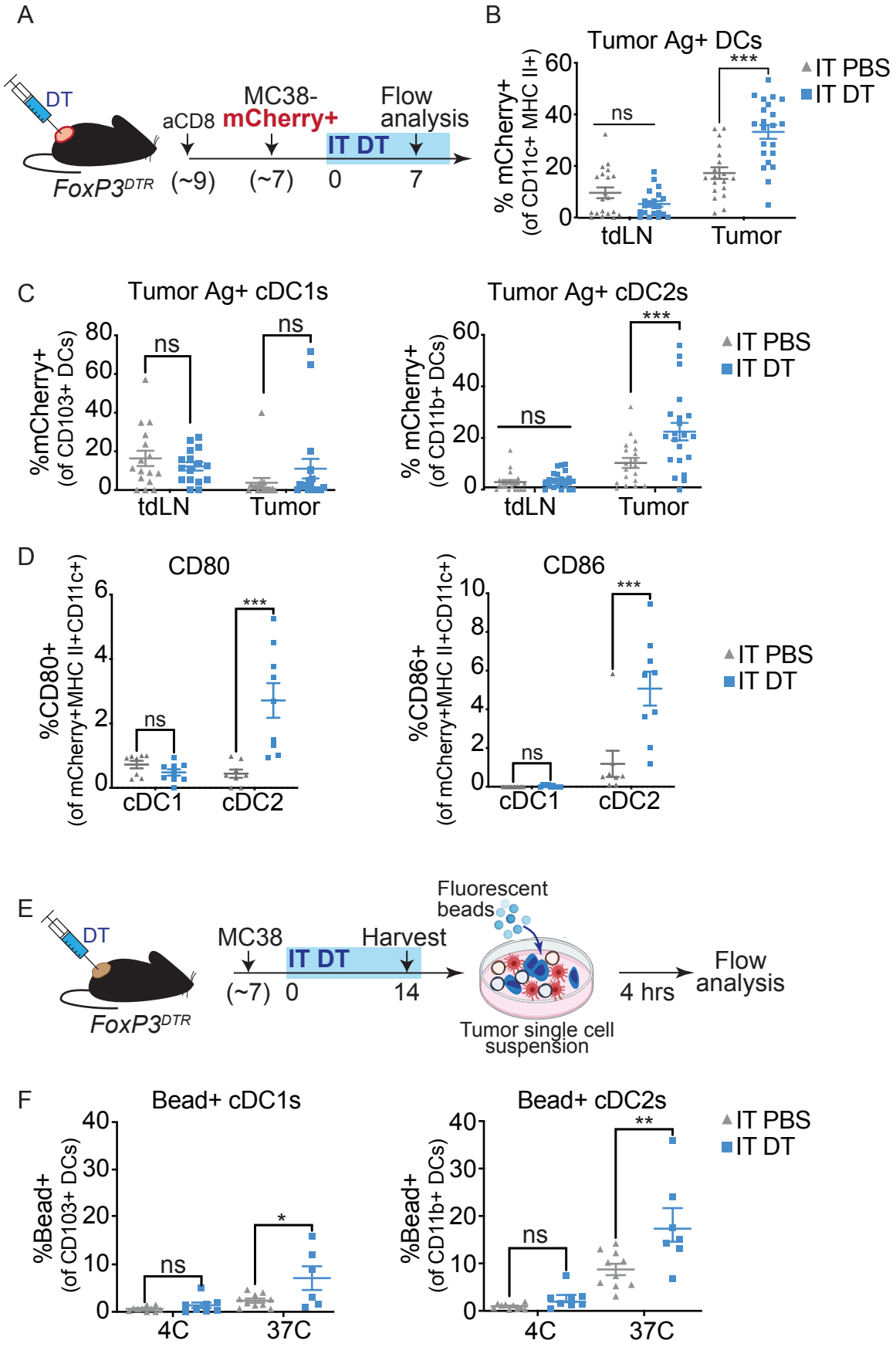
A
DT
FoxP3DTR
aCD8
MC38-
mCherry+
Flow
analysis
IT DT
(~9)
(~7)
0
7
B
Tumor Ag+ DCs
% mCherry+
(of CD11c+ MHC II+)
ns
***
tdLN
Tumor
IT PBS
IT DT
C
Tumor Ag+ cDC1s
%mCherry+
(of CD103+ DCs)
Tumor Ag+ cDC2s
% mCherry+
(of CD11b+ DCs)
D
CD80
%CD80+
(of mCherry+MHC II+CD11c+)
CD86
%CD86+
(of mCherry+MHC II+CD11c+)
cDC1
cDC2
E
MC38
Harvest
Fluorescent
beads
Tumor single cell
suspension
4 hrs
Flow
analysis
F
Bead+ cDC1s
%Bead+
(of CD103+ DCs)
Bead+ cDC2s
%Bead+
(of CD11b+ DCs)
4C
37C
*
**

Figure 7. IT Treg ablation enhances tumor antigen acquisition by cDC2s.
(A)Experimental schematic. *Foxp3*^{DTR} mice received anti-CD8 depleting antibodies two days prior to mCherry+ MC38 tumor inoculation and every six days thereafter. IT DT began when tumors reached 50mm^3.
(B) Quantification of mCherry+ DCs after IT PBS or IT DT treatment.
(C) Quantification of mCherry+ cDC1s or cDC2s in tumor and tdLNs.
(D) Quantification of CD80 and CD86 expression on mCherry+ cDC1s and mCherry+ cDC2s.
(E) Schematic of experimental approach in *ex vivo* assays. *Foxp3*^{DTR} mice were inoculated with MC38 tumors and dosed with IT DT when tumors reached 50mm^3. Tumors were harvested and plated with fluorescent beads after seven days of IT DT treatments.
(F) Frequencies of cDC1s or cDC2s that phagocytosed beads at either 4C or 37C.
In vivo data are representative of 2 independent experiments. *Ex vivo* data are representative of 3 independent experiments. Data represent means ± SEM; *$p < 0.05$, **$p < 0.01$ and ***$p < 0.001$. B-E; G,H: Ordinary two-way ANOVA with Tukey's multiple comparison test. (n=4-7 mice/group).